Am J Cancer Res 2020;10(3):816-837
www.ajcr.us /ISSN:2156-6976/ajcr0108362

Original Article

α1,6-Fucosyltransferase (FUT8) regulates the cancer-promoting capacity of cancer-associated fibroblasts (CAFs) by modifying EGFR core fucosylation (CF) in non-small cell lung cancer (NSCLC)

Fengzhou Li[1*], Shilei Zhao[1*], Yanwei Cui[3*], Tao Guo[1], Jiaqi Qiang[5], Qiang Xie[1], Wendan Yu[2], Wei Guo[2], Wuguo Deng[4], Chundong Gu[1], Taihua Wu[1]

[1]The First Affiliated Hospital, [2]Institute of Cancer Stem Cell, Dalian Medical University, Dalian, China; [3]Zhongshan Hospital, Dalian University, Dalian, China; [4]Sun Yat-sen University Cancer Center, State Key Lab of Oncology in South China, Guangzhou, China; [5]Dalian Municipal Central Hospital Affiliated to Dalian Medical University, Dalian, China. [*]Equal contributors.

Received January 26, 2019; Accepted February 28, 2020; Epub March 1, 2020; Published March 15, 2020

Abstract: Cancer-associated fibroblasts (CAFs) are the main cancer-promoting component in the tumor microenvironment (TME) of non-small cell lung cancer (NSCLC). α1,6-Fucosyltransferase (FUT8), the key enzyme catalyzing core α1,6-fucosylation (CF), plays a promoting role in multiple malignancies. In the current study, we investigated the function of FUT8 in CAFs and elucidated the mechanism through which FUT8 regulates the cancer-promoting capacity of CAFs in NSCLC. A bioinformatics analysis was performed to reveal the relationship between FUT8 and CAFs. Resected specimens from NSCLC patients were analyzed to assess the expression of FUT8 in CAFs. Primary CAFs and normal lung fibroblasts (NLFs) were extracted from NSCLC patient specimens and were co-cultured with NSCLC cell lines in a novel 3D-printed non-contact co-culture device. An In vivo CAF/NSCLC co-injection tumorigenesis assay was performed using nude mice to study the function of FUT8/CF in TME formation. The current study revealed that FUT8-mediated CF in CAFs plays a positive role in the cancer-promoting capacity of these cells. FUT8 overexpression was observed in CAFs isolated from some lung adenocarcinoma cases. Further investigation showed that FUT8/CF in CAFs promoted the formation of an invasive and malignant TME in vivo and in vitro, and the resulting NSCLC cells exhibited faster proliferation and increased invasiveness. EGFR signaling exerts a catalytic effect on the cancer-promoting capacity of CAFs and is regulated by the CF modification of the EGFR protein.

Keywords: Cancer-associated fibroblasts, α1,6-fucosyltransferase, non-small cell lung cancer, tumor microenvironment, epidermal growth factor receptor

Introduction

Lung cancer is the most common malignancy in the world [1], and non-small cell lung cancer (NSCLC) accounts for approximately 85% of lung cancer cases [2]. Due to the presence of micrometastasis, even early-stage patients are at risk of metastasis and relapse after radical treatment [3]. Therefore, the mechanism of NSCLC proliferation and metastasis still needs to be further explored, and more effective molecular therapeutic targets need to be identified.

In recent years, the crosstalk between the tumor microenvironment (TME) and cancer cells has received increasing attention [4]. Cancer-associated fibroblasts (CAFs), the most abundant component of the TME, account for 70% of the cells in solid tumors [5]. CAFs are most often identified by the expression of specific biomarkers such as α-smooth muscle actin (α-SMA) [6], fibroblast activation protein (FAP), and vimentin [7]. As demonstrated by major studies, the transformation of normal lung fibroblasts (NLFs) to a myofibroblast phenotype and their subsequent acquisition of cancer-associated properties results in the formation of CAFs. CAFs can promote tumor progression through direct interaction and the secretion of various cytokines [8]. Thus, elucidation of the mecha-

nisms underlying the activation and maintenance of CAFs could lead to novel therapeutic approaches.

Glycosylation, a common type of posttranslational protein modification, is essential for many of the biological functions of glycoproteins [9]. Fucosylation catalyzed by fucosyltransferases is one of the most common forms of glycosylation [10]. FUT8, which is also known as α1,6-fucosyltransferase, is the only enzyme that catalyzes the core α1,6-fucosylation (CF) in mammals [11]. FUT8 is responsible for the transfer of a fucosyl moiety to glycoproteins via an α1,6 linkage to generate the CF modification [12]. This modification is essential for the development and progression of cancer [9, 13-17]. However, whether FUT8/CF plays a role in the TME remains unknown.

Epidermal growth factor receptor (EGFR, ErbB1), a member of the ErbB receptor family, has received much attention due to its strong association with malignant proliferation [18]. EGFR serves as a mediator of cell signaling by extracellular growth factors to activate intracellular pathways, such as the PI3K/AKT/mTOR, JAK/STAT, and MAPK/ERK pathways [19]. The CF modification of EGFR is essential for the activation of EGFR via tyrosine phosphorylation [20-22]. The deregulation of EGFR signaling is commonly observed in CAFs [23-25]. For example, EGFR signaling is reportedly relevant to the cancer-promoting ability of CAFs in breast cancer [23]. Extracellular ligands of EGFR such as epidermal growth factor (EGF) [26, 27], transforming growth factor-alpha (TGF-α) [28], neuregulin1 (NRG1) [29] and G protein estrogen receptor (GPER) [23] had also been found to be essential for the activation and maintenance of CAFs.

Our previous study showed that FUT8/CF is responsible for the transformation of pericytes into myofibroblasts in pulmonary fibrosis [30], and this process is very similar to that underlying the activation of NLFs toward CAFs. In the current study, FUT8 overexpression was observed in the tumor stroma of six out of eight lung adenocarcinoma cases and in CAFs from three out of five lung adenocarcinoma cases. In vitro and in vivo assays confirmed that FUT8/CF was crucial to the cancer-promoting capacity of CAFs. We also identified EGFR as a protein controlled by FUT8/CF that played a role in the cancer-promoting capacity of CAFs.

Materials and methods

Oncomine database

We performed data mining using Oncomine (https://www.oncomine.org/), which is the world's largest gene chip database. The datasets were searched using the following filters: ① Gene: FUT8; ② Analysis: Cancer vs. Normal Analysis; ③ Cancer Type: Lung Cancer; ④ Data Type: mRNA or DNA Copy Number; ⑤ *p*-value: 0.05; ⑥ Fold Change: 1.5; ⑦ and Gene Rank: 10%. The method used for data analysis was based on previous articles [31-33]. The differences in gene expression values between groups were assessed through a t-test.

Patient characteristics and tissue preparation

Specimens from 10 patients with definitive p-stage III lung adenocarcinoma were collected at the First Affiliated Hospital of Dalian Medical University in 2018 (Dr. Fengzhou Li and Dr. Tao Guo). Paired normal lung tissues for each tumor (collected 4~5 cm from the incisal margin) was were simultaneously obtained. The staging of these patients was based on the *8th Edition International Union Against Cancer/American Joint Committee on Cancer TNM Classification* [34]. The study was approved by the Medical Ethical Committees of the First Affiliated Hospital of Dalian Medical University. All specimens were obtained from primary lesions. Two small pieces (0.25 cm^3) of tissue were resected from each sample and were prepared for the extraction of total cellular proteins and the culture of primary fibroblasts. The rest of the samples were fixed with formalin, embedded with paraffin, and continuously sliced to a thickness of 4 μm.

Immunohistochemistry (IHC) staining and evaluation of the protein expression levels

A streptavidin-peroxidase staining kit was purchased from ZSGB BIO (Beijing, China). IHC staining of FUT8 and α-SMA was performed according to the manufacturer's instructions for the products used in our previous studies [35, 36]. 3,3'-Diaminobenzidine (DAB) staining was performed, and the results were observed under a microscope. Pathological diagnosis

was performed according to the *2015 World Health Organization Classification of Lung Tumors* [37] and the *International Association for the Study of Lung Cancer/American Thoracic Society/European Respiratory Society International Multidisciplinary Classification of Lung Adenocarcinoma* [38]. The CAFs were clearly marked by α-SMA, and the same position of a serial slice can then be analyzed using previously reported methodologies for evaluating protein levels in CAFs [39-43] to determine the expression of FUT8 in CAFs.

Culture of primary fibroblasts

A small piece (0.25 cm^3) of each tissue was resected, soaked in Dulbecco's modified Eagle medium (DMEM) at 0°C and digested within 2 h in the laboratory. Tumor tissues and paired normal lung tissues (collected 4~5 cm from the incisal margin) were homogenized and digested for 2.5~4 h at 37°C in DMEM containing 0.1 mg/mL Roche DNase I (Basel, Switzerland) and 1 mg/mL Roche collagenase A. The cells were filtered through a 75 μm filter and resuspended and plated with DMEM containing 1% penicillin/streptomycin and 15% GIBCO fetal bovine serum (FBS, Massachusetts, US). The cultures were maintained at 37°C in 5% CO_2. After five passages, the cell purity was tested by RT-PCR. The CAFs were then immortalized with the SV40-large T antigen (EX-SV40T-Lv105, GeneCopoeia/Funeng, Guangdong Province, China) following the recommended protocol. Finally, five paired primary fibroblast cell lines were successfully extracted and cultured in DMEM containing 1% penicillin/streptomycin and 10% FBS. CAFs were continuously co-cultured with A549 or H322 cells to maintain their cancer-associated phenotype. All CAFs used for experiments were co-cultured with NSCLC cells for at least five continuous passages.

Cell lines and in vitro cell culture

We selected A549, H322, and human lung fibroblast (HLF) cells for in vitro experiments due to their satisfactory growth in DMEM, which allows easier observation of their interactions in the co-culture system. The human NSCLC cell lines A549 and H322 were obtained from The American Type Culture Collection (ATCC, Virginia, US). The human lung fibroblast cell lines HLF, MRC5, and HFL1 were gifts from the Institute of Cancer Stem Cells of Dalian Medical University. All cell lines were cultured in DMEM containing 1% penicillin/streptomycin and 10% FBS at 37°C under 5% CO_2.

Noncontact co-culture system

A non-contact co-culture device was designed (already undergoing the patent examination and approval process in China) and generated by 3D printing (Wanwan 3D, Guangdong Province, China) using highly transparent non-toxic resin. The reliability of the device was verified in a recent study [44]. The schematic diagram of the device used for 3D printing is shown in **Figure 4F**, and a modified version that was easier to produce was used in this study (Supplementary Figure 1C). The device was a vessel consisting of two culture wells and one precipitation well. The culture wells and the precipitation well were separated by two 2-mm-high partitions. During cell seeding, the liquid levels in both culture wells should not exceed the height of the partition. Fibroblasts and NSCLC cells were seeded into the two culture wells at a ratio of 2:1. After cell adherence, DMEM containing 10% FBS was added to the vessel until the liquid level exceeded the height of the partition. Based on the design of the co-culture device, floating cells do not directly enter the contralateral culture well but are deposited into the precipitation well. Before the cells were manipulated in any way, the medium in the precipitation well was drained in case any floating cells had entered the contralateral culture well. The two cell lines were then isolated again, and 0.5% trypsin was used for the separate passage/collection of the two cell lines.

Conditioned medium (CM)

Fibroblasts were cultured in DMEM with 10% FBS and routine antibiotics. When the cells reached 80% confluence, the medium was changed to FBS-free medium. After 48 h, the supernatant was extracted and centrifuged at 1600×g for 10 minutes. The CM was stored at -80°C and used for the colony formation assay.

Reagents and antibodies

Primary antibodies against α-SMA and FUT8 were purchased from Abcam (Cambridge, UK). Another primary antibody against FUT8 was purchased from Proteintech (Hubei Province,

China). Primary antibodies against EGFR, β-actin, and ST6Gal1 were also purchased from Proteintech (Hubei Province, China). A primary antibody against p-EGFR was purchased from Santa Cruz (Texas, USA). A primary antibody against Twist was purchased from Wanleibio (Liaoning Province, China). Primary antibody kits for epithelial-mesenchymal transition (EMT) markers (9782, against N-cadherin, vimentin, Slug, Snail, β-catenin, and E-cadherin), the G1/S cell cycle checkpoint (9870 and 9932, against CDK2, p-CDK2, CDK4, CDK6, Cyclin-E2, Cyclin-D1, Cdc25A, and P21), the MAPK/ERK1/2 pathway (9910, 9911, 9916 and 9926, against p53, c-Raf, p-c-Raf, MEK1/2, p-MEK1/2, ERK1/2, and p-ERK1/2, respectively), the phospho-Jak family (97999T, against p-JAK), and p-Akt (Thr308) were purchased from Cell Signaling Technology (Massachusetts, USA). Biotinylated *Lens culinaris agglutinin* (LCA), a lectin that can specifically identify fucose, was purchased from Vector Labs (California, USA). NSC 228155, an activator of EGFR that binds to the extracellular region of EGFR and enhances tyrosine phosphorylation of EGFR, was purchased from MedChemExpress (New Jersey, USA). Other chemicals and reagents were purchased from Sigma (Missouri, USA) and Vetec (St. Louis, USA).

Plasmids and lentiviruses

Four mCherry-labeled shRNA fragments targeting the FUT8 gene, one GFP labeled expression clone fragment encoding the full-length FUT8 ORF, and the corresponding negative control vectors were purchased from GeneCopoeia. The sequences of the shRNAs were as follows: sh1 5'-GCCGAGAACTGTCCAAGATTC-3', sh2 5'-GCGGAGAATAACATATCTTCA-3', sh3 5'-GGTGTGTAATATCAACAAAGG-3', and sh4 5'-GCTTCAAACATCCAGTTATTG-3'. Lentiviral particles were generated based on a standardized protocol using highly purified plasmids and EndoFectin-Lenti and TiterBoost reagents. Viral packaging was conducted based on recommended protocols and previous reports. The lentiviral expression construct was validated by full-length sequencing, restriction enzyme digestion, and PCR-size validation using gene-specific and vector-specific primers. Four shRNA fragments targeting the EGFR gene were obtained from the Human GIPZ shRNA Bank of Dalian Medical University. The sequences of the shRNAs were as follows: sh1 5'-AGGAACTGGATATTCTGAA-3', sh2 5'-AGATCAGAAGACTACAAAA-3', sh3 5'-TGGTGTGTGCAGATCGCAA-3', and sh4 5'-ACGAATATTAAACACTTCA-3'. The stable shEGFR-expressing cell line was generated according to our previous reports [45, 46].

RNA extraction and RT-PCR.

Total RNA from CAFs and their paired NLFs was extracted using the TRIzol method according to previous reports [47]. A TransScript One-step gDNA Removal and cDNA Synthesis Supermix purchased from Transgene (Beijing, China) was used to synthesize the first-strand cDNA. Taq Master Mix (Vazyme, Nanjing, China) was used for quantitative PCR according to the manufacturer's instructions. The reaction program was set according to the Tm values of the primers. The primer sequences were as follows: vimentin-F 5'-TGCCGTTGAAGCTGCTAACTA-3', vimentin-R 5'-CCAGAGGGAGTGAATCCAGATTA-3', FAP-F 5'-ATGAGCTTCCTCGTCCAATTCA-3', FAP-R 5'-AGACCACCAGAGAGCATATTTTG-3', α-SMA-F 5'-ATTGCCGACCGAATGCAGA-3', and α-SMA-R 5'-ATGGAGCCACCGATCCAGAC-3'.

Western blot analysis and lectin blot analysis

Total protein was collected according to the methods described in our previous report [35]. The protein concentration of the cell lysis solution was assessed using a Thermo Fisher BCA kit. Subsequently, 20~30 μg of total protein was separated by 10% SDS-PAGE and transferred to a polyvinylidene fluoride (PVDF) membrane. The samples were incubated with primary antibodies diluted to the recommended concentration overnight at 4°C. The samples were incubated with an HRP-conjugated secondary antibody at room temperature for 2 h, and the protein bands were detected using a chemiluminescence device. The lectin blot protocol was similar to that used for the western blot analysis with the exception that biotinylated *LCA* was used instead of the primary antibodies.

Colony formation assay

A549 or H322 cells were seeded in six-well plates (2×10^3 cells per well) and incubated in complete DMEM for 24 h. The medium was then replaced by CM with 10% FBS, and the cells were cultured in an incubator at 37°C with

5% CO_2 for 2 weeks until they grew into colonies. The medium was subsequently removed, and the cell colonies were stained with 0.1% crystal violet and counted.

Transwell assay

After five continuous co-culture passages, cell migration and invasion assays were performed in Transwell chambers with a pore size of 8.0 μm (Corning, NY, USA). The cells were starved overnight in FBS-free DMEM, collected and resuspended. A total of 1×10^5 A549 or H322 cells were resuspended in 250 μL of DMEM with 10% FBS and injected into the upper chamber. A total of 3×10^5 CAFs (or other fibroblasts) were resuspended in 500 μL of DMEM with 10% FBS and injected into the lower chamber. In the invasion assay, 70 μL/well of Matrigel (Corning, NY, US) diluted with DMEM at a ratio of 1:5 was added to the upper chambers before the experiment. Twenty-four hours after cell seeding, the upper chambers were washed with PBS and dried at RT. The migrated or invaded cells on the backside of the Transwell membranes were stained with 0.1% crystal violet, and the number of cells was recorded under a microscope.

Cell cycle analysis

After five continuous co-culture passages, the cells were trypsinized, washed with PBS, resuspended in chilled methanol, and maintained overnight at -20°C. Each cell sample was resuspended in 500 μL of buffer containing 480 μL of PBS, 5 μL of RNase, 5 μL of PI and 10 μL of Triton X-100 and incubated at 37°C for 30 min. After centrifugation, the cells were resuspended in PBS and filtered. Cell cycle analysis was performed using a FACS Caliber Flow Cytometer (BD Biosciences, California, US).

Lectin fluorescence

Cells grown on chamber slides were washed with PBS and fixed with 4% paraformaldehyde for 15 min at room temperature. The samples were pretreated with Triton X-100 and incubated with 10% BSA in PBS for 30 min. Red luminous LCA was added, and the mixture was incubated at room temperature for 1 h. DAPI was added to stain the nuclei. The samples were examined with a fluorescence microscope.

Immunoprecipitation (IP) assay

Lysates of fibroblasts were mixed with anti-EGFR or IgG antibodies and placed overnight on table shaker at 4°C. Forty micrograms protein A/G magnetic nanospheres (Santa Cruz, Texas, USA) were added to the mixture, and the resulting mixture was shaken at 4°C for 4 h. EGFR proteins were extracted following recommended protocols and analyzed by a lectin blot, as described above.

In vitro co-culture assay

Because co-injection tumorigenesis requires an appropriate mixing ratio of cell components, an in vitro co-culture assay was conducted before the co-injection. GTP (green)-labeled CAFs and mCherry (red)-labeled A549 cells were combined in test tubes and seeded in 10 cm dishes for direct contact co-culture. After continuous co-culture for five passages, the cells were observed under a fluorescence microscope. The final cell ratios were calculated as a reference to select the initial cell ratio for in vivo co-injection.

Subcutaneous co-injection tumorigenesis in nude mice

Twenty-one female BALB/c nu+/nu+ nude mice aged 4 to 6 weeks were purchased and housed in the *specific pathogen-free animal center at Dalian Medical University* and were divided randomly into three groups with seven mice in each group. All procedures involving mice were approved by the Committee for the Care and Use of Laboratory Animals of Dalian Medical University. In this model system, fibroblasts (CAFs-NC, CAFs-shFUT8, or HLFs-NC) were mixed with epithelial cells (A549). CAFs and A549 cells were mixed at a ratio of 2:1, cast in Matrigel (a tota of 5×10^5 cells in 100 μL of gel), and subcutaneously injected into the left flank of each mouse. The tumor sizes and weights of the mice were examined every seven days after injection. The recombinant tissues were retrieved after a designated period of time (28 days) and analyzed.

Bioinformatics and gene enrichment analyses

The data used in the study were obtained from the GSE22862 gene chip data in the NCBI Gene Expression Omnibus (GEO). This gene chip contains the genome data of 15 primary CAF cell lines extracted from NSCLC cases. The differential expression of genes was calculated using the R package limma. The genes that were significantly coexpressed with the FUT8

gene (P<0.05) were subjected to enrichment analysis using the R package Cluster-Profiler.

Results

FUT8 is overexpressed in the CAFs of most lung adenocarcinoma cases

To investigate whether FUT8 is overexpressed in lung cancer, we analyzed gene expression data obtained from the Oncomine database. Eighty-nine datasets in Oncomine that contained significant expression data for FUT8 were searched, and 73 of these 89 (82%) datasets suggested that FUT8 was overexpressed in cancer. Seven of these 89 datasets showed that FUT8 was overexpressed in lung cancer (**Figure 1A**). As shown in **Figure 1B-H**, all seven datasets indicated that FUT8 was overexpressed in lung adenocarcinoma tissue compared with normal lung tissue (1.626~2.569 fold higher expression compared with that in normal lung tissues). The names and reporter IDs of the seven datasets are provided in the corresponding figures to allow researchers to easily find these datasets and repeat our analysis.

To confirm the above-mentioned findings, we found higher FUT8 protein expression in tumor tissues compared with adjacent normal tissues from 10 patients with lung adenocarcinoma (**Figure 1I**). We then assessed the expression of FUT8 in CAFs in different pathological subtypes of lung adenocarcinoma tissues by IHC. As shown in **Figure 1J**, the tumor stroma was clearly marked by α-SMA, and the expression of FUT8 in CAFs was evaluated in the same position of a serial slice. However, as shown in Supplementary Figure 1A, we found that it was impossible to mark the borders between stromal cells and cancer cells in a solid predominant adenocarcinoma (SPA, Patient 04) and a mucinous adenocarcinoma (MUC, Patient 05). The analysis of the other eight cases revealed that FUT8 was overexpressed in the tumor stroma in six cases and in adjacent normal tissue in one case. The above results showed that FUT8 was overexpressed not only in lung adenocarcinoma cells but also in the tumor stroma.

FUT8 is overexpressed in CAFs and mediates high levels of CF

To obtain purified CAFs for subsequent research, we attempted to extract and culture primary CAF/NLF cell lines in vitro from the 10 lung adenocarcinoma cases. Five pairs of CAFs/NLFs were successfully isolated from five patients (P01, P03, P06, P07, and P08), but we failed to isolate paired fibroblasts from the other five patients (P02 P04, P05, P09, and P10). No morphological difference between primary CAFs and NLFs could be observed under a microscope (Supplementary Figure 1B).

The primary fibroblasts were subsequently identified by specific myofibroblast markers (α-SMA, FAP, and vimentin). The mRNA expression levels of α-SMA and FAP in CAFs were significantly higher than that in NLFs, and the expression of vimentin mRNA in CAFs was slightly higher than that in NLFs. In general, CAFs exhibited a myofibroblastic phenotype compared with NLFs (**Figure 2A**). A western blot analysis showed that FUT8 protein was overexpressed in three out of five CAFs (P03, P07, and P08 compared with each paired NLF) (**Figure 2B**). A lectin blot analysis (using LCA to detect fucose) showed a consistent result: the binding of fucose to total cellular proteins was up-regulated in the CAFs obtained from P03, P07, and P08 (**Figure 2C**).

To select a proper cell line that can serve as a control for CAFs, the expression of α-SMA, FUT8, and ST6Gal1 (the key enzyme for sialic acid glycosylation) were tested by western blot in CAFs and three laboratory-grown human lung fibroblast cell lines (MRC5, HLF1, and HLF) was assessed by western blot analysis. HLFs exhibited the lowest α-SMA, FUT8, and ST6Gal1 expression compared with CAFs (**Figure 2D**, **2E**). Thus, HLF cells were selected as a control cell line for CAFs. Next, lectin fluorescence assays (using LCA to detect fucose) were performed using primary CAFs, primary NLFs, and lab-grown HLFs. The results showed taht the fucose modification in the cytoplasm of CAFs was significantly higher than that in the cytoplasm of NLFs and HLFs (**Figure 2F**).

FUT8 in CAFs is necessary for the construction of an invasive TME in vivo

We selected the CAFs from the cases P03, P07, and P08 for further experiments. Four shRNA fragments were used to down-regulate FUT8 in CAFs, and the effects were tested by western blot (**Figure 3A**). Sh4 was used to establish a stable CAF-shFUT8 cell line, and a lectin blot

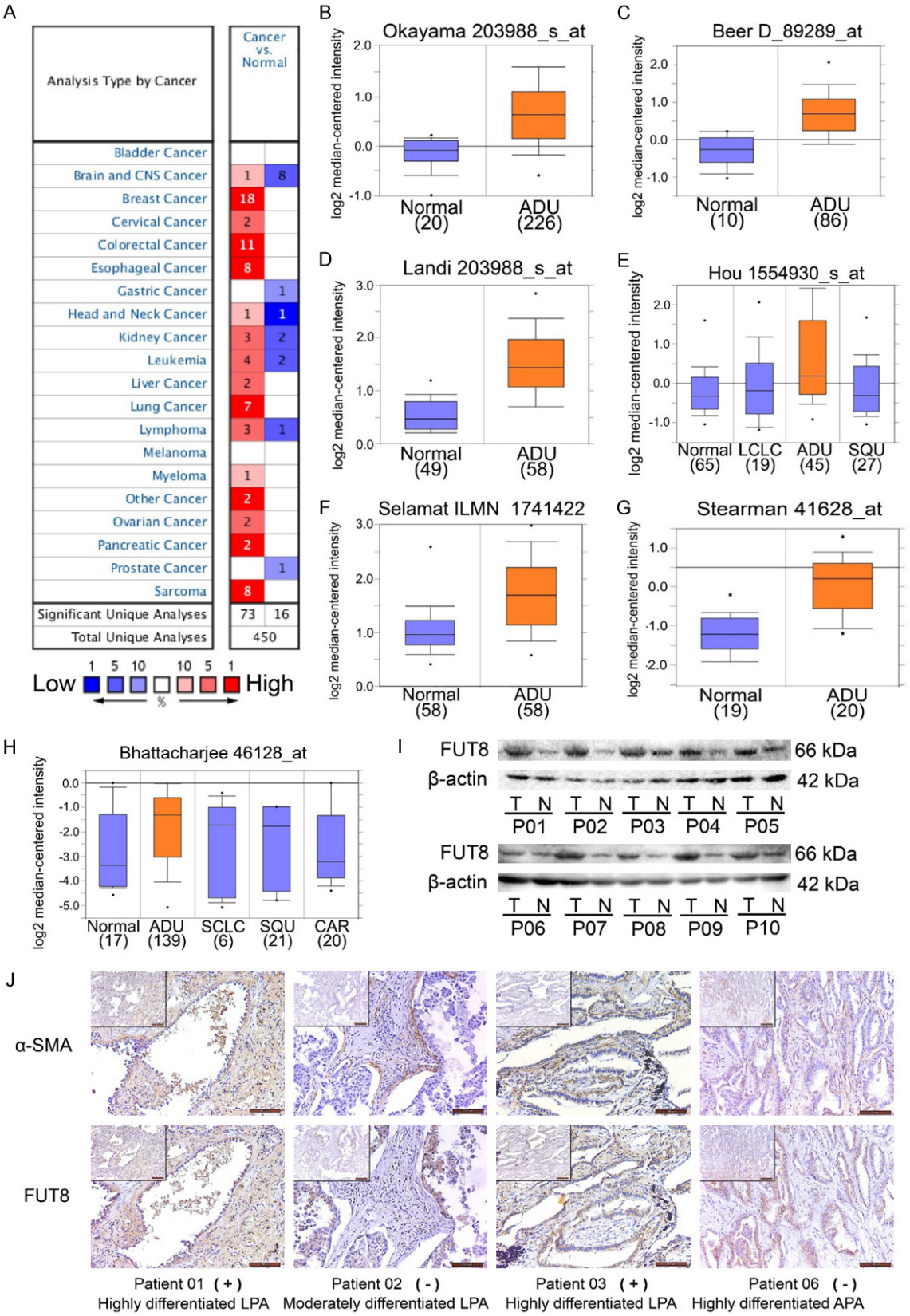
A
Analysis Type by Cancer
Cancer vs. Normal
Bladder Cancer
Brain and CNS Cancer 1 8
Breast Cancer 18
Cervical Cancer 2
Colorectal Cancer 11
Esophageal Cancer 8
Gastric Cancer 1
Head and Neck Cancer 1 1
Kidney Cancer 3 2
Leukemia 4 2
Liver Cancer 2
Lung Cancer 7
Lymphoma 3 1
Melanoma
Myeloma 1
Other Cancer 2
Ovarian Cancer 2
Pancreatic Cancer 2
Prostate Cancer 1
Sarcoma 8
Significant Unique Analyses 73 16
Total Unique Analyses 450
Low 1 5 10 10 5 1 High
%
B
Okayama 203988_s_at
log2 median-centered intensity
Normal (20)
ADU (226)
C
Beer D_89289_at
Normal (10)
ADU (86)
D
Landi 203988_s_at
Normal (49)
ADU (58)
E
Hou 1554930_s_at
Normal (65)
LCLC (19)
ADU (45)
SQU (27)
F
Selamat ILMN 1741422
Normal (58)
ADU (58)
G
Stearman 41628_at
Normal (19)
ADU (20)
H
Bhattacharjee 46128_at
Normal (17)
ADU (139)
SCLC (6)
SQU (21)
CAR (20)
I
FUT8
66 kDa
β-actin
42 kDa
T N
P01 P02 P03 P04 P05
P06 P07 P08 P09 P10
J
α-SMA
FUT8
Patient 01 (+) Highly differentiated LPA
Patient 02 (-) Moderately differentiated LPA
Patient 03 (+) Highly differentiated LPA
Patient 06 (-) Highly differentiated APA

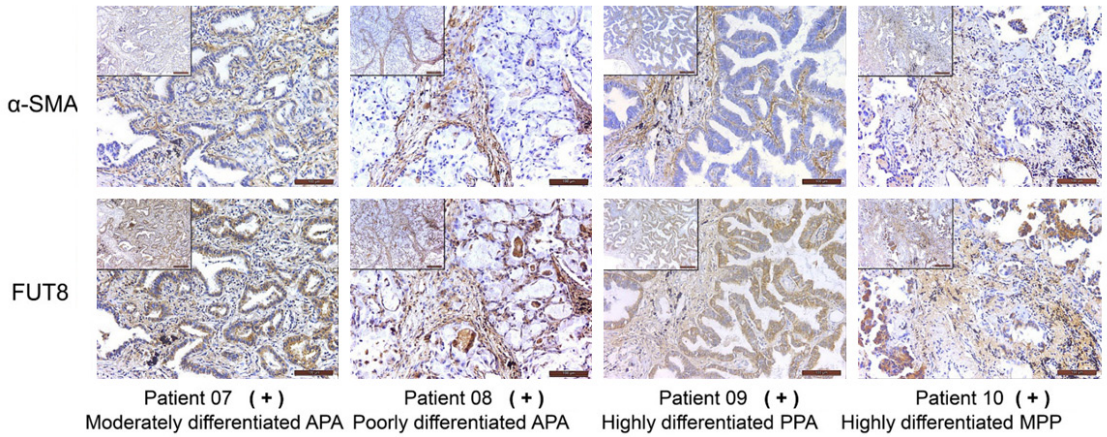

Figure 1. FUT8 is overexpressed in CAFs of most adenocarcinoma cases. A. Cancer type analysis of the 89 significant datasets in Oncomine. Red: overexpression. Blue: low expression. B-H. FUT8 levels across cancer/normal tissues in the seven significant data sets. The sample size of each group is marked in brackets. ADU: lung adenocarcinoma. SCLC: small cell lung cancer. SQU: squamous cell lung carcinoma. CAR: lung carcinoid tumor. LCLC: large cell lung cancer. I. FUT8 protein expression in 10 pairs of NSCLC and normal tissues was tested by western blot analysis. T: tumor tissue. N: normal lung tissue. J. α-SMA and FUT8 protein expression in serial slices of lung adenocarcinoma tissues was tested by IHC. Representative images are shown. LPA: lepidic predominant adenocarcinoma. APA: acinar predominant adenocarcinoma. PPA: papillary predominant adenocarcinoma. MPP: micropapillary predominant adenocarcinoma. Scale bar: 100 μm.

analysis showed that the CF levels were down-regulated in CAF-shFUT8 cells (**Figure 3B**).

To investigate the proper ratio for the cell mixture in the subcutaneous co-injection tumorigenesis assays performed using nude mice, we conducted an in vitro co-culture assay. According to the results, a CAFs: A549 cells ratio of 2:1, which stably mimicked a TME similar to that found in primary lung cancer, was selected as the initial ratio for subcutaneous co-injection into nude mice (**Figure 3C**). During the period used for the observation of tumorigenesis, the changes in body weight and tumor diameters were recorded. As shown in **Figure 3D**, **3E**, the growth of CAF-NC/A549 tumors was significantly faster than that of CAF-shFUT8 and HLF-NC/A549 tumors. However, the change in body weight of the mice showed no significant difference among the three groups. After 28 days, the tumors were removed (**Figure 3F**), and the final weights of the tumors are shown in **Figure 3G**. The final volume and weight of the tumors generated by CAFs-NC/A549 cells were significantly higher than those of the tumors generated by CAFs-shFUT8/A549 and HLF-NC/A549 cells. The results indicated that FUT8 expression in CAFs had a marked promoting effect on tumor formation and growth.

Next, the tumor stroma was marked with IHC staining of α-SMA. Interestingly, NSCLC cells showed increased invasiveness into the stroma in tumors generated by CAF-NC/A549 cells. Conversely, NSCLC cells rarely invaded the stroma in tumors generated by CAF-shFUT8/A549 or HLF-NC/A549 cells. In the CAF-shFUT8/A549- and HLF-NC/A549-generated tumors, NSCLC cells preferred to clump together and formed a clear boundary with the tumor stroma (**Figure 3H**).

CF mediated by FUT8 is necessary for the cancer-promoting capacity of CAFs

FUT8 was stably up-regulated in HLF cells using a lentivirus packed FUT8 ORF sequence (**Figure 4A**). A lectin (LCA) blot analysis showed that the binding of fucose to total cellular proteins was also up-regulated in HLF-FUT8 overexpressing (OE) cells (**Figure 4B**). To investigate the effect of FUT8 in CAFs on tumor proliferation, we treated A549 and H322 cells with CM from fibroblasts (CAFs-NC, CAFs-shFUT8, HLFs-FUT8 OE, and HLFs-NC) prior to clone formation assays. The result showed that the down-regulation of FUT8 in CAFs reduced the ability of CAFs to increase the proliferation rate of tumor cells, whereas the up-regulation of FUT8 in HLFs slightly increased this ability (**Figure 4C**). Migration and invasion assays showed that the down-regulation of FUT8 in CAFs reduced the migration and invasion of co-cultured NSCLC cells, whereas the up-regulation of FUT8 in

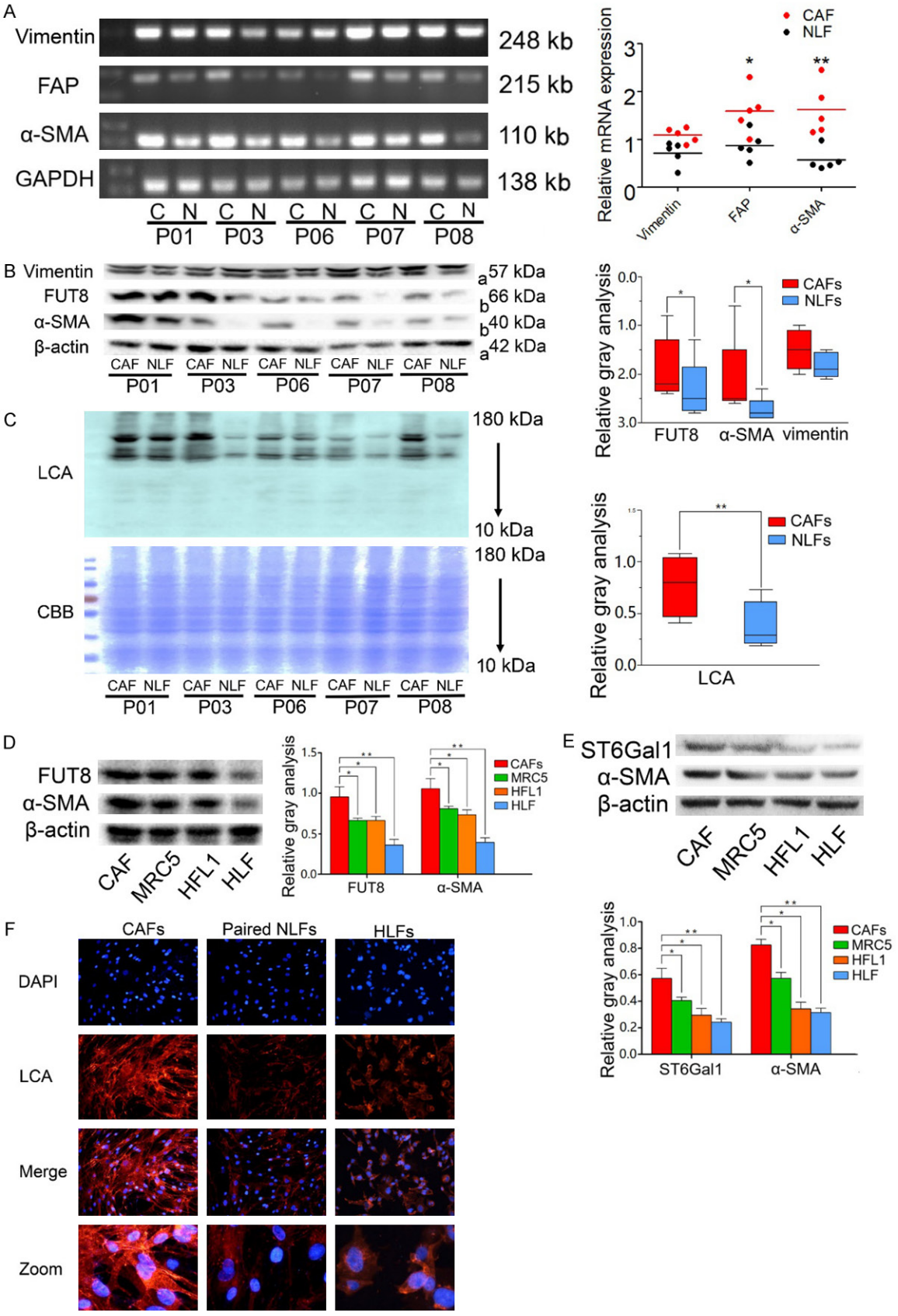
A
Vimentin
FAP
α-SMA
GAPDH
248 kb
215 kb
110 kb
138 kb
C N C N C N C N C N
P01 P03 P06 P07 P08
CAF
NLF
Relative mRNA expression
Vimentin
FAP
α-SMA
B Vimentin
FUT8
α-SMA
β-actin
a57 kDa
b66 kDa
b40 kDa
a42 kDa
CAF NLF CAF NLF CAF NLF CAF NLF CAF NLF
P01 P03 P06 P07 P08
CAFs
NLFs
Relative gray analysis
FUT8
α-SMA
vimentin
C
LCA
CBB
180 kDa
10 kDa
180 kDa
10 kDa
CAF NLF CAF NLF CAF NLF CAF NLF CAF NLF
P01 P03 P06 P07 P08
CAFs
NLFs
Relative gray analysis
LCA
D
FUT8
α-SMA
β-actin
CAF
MRC5
HFL1
HLF
Relative gray analysis
FUT8
α-SMA
CAFs
MRC5
HFL1
HLF
E
ST6Gal1
α-SMA
β-actin
CAF
MRC5
HFL1
HLF
Relative gray analysis
ST6Gal1
α-SMA
CAFs
MRC5
HFL1
HLF
F
CAFs
Paired NLFs
HLFs
DAPI
LCA
Merge
Zoom

Figure 2. FUT8 is overexpressed in CAFs and mediates high levels of CF. A. Myofibroblast markers in the total mRNA of the five pairs of primary fibroblasts were tested by RT-PCR. C: CAFs. N: NLFs. B. The expression of myofibroblast markers and FUT8 in primary CAFs and paired NLFs were tested by western blot analysis. Protein bands with the same subscript letter were transferred from the same SDS-PAGE gel. C. The CF levels in the primary CAFs and paired NLFs were tested by lectin bolt analysis. LCA: *Lens culinaris agglutinin*. CBB: Coomassie brilliant blue. D. FUT8 and α-SMA expression in CAFs and laboratory-grown normal fibroblasts was tested by western blotting. E. ST6Gal1 and α-SMA expression in CAFs and laboratory-grown normal fibroblasts was tested by western blot analysis. F. The CF levels of CAFs, NLFs, and HLFs were tested via lectin fluorescence. Magnification: 400×/800×. All experiments were repeated three times.

HLFs only slightly enhanced the migration of H322 cells (**Figure 4D**, **4E**).

Next, cell apoptosis and cell cycle assays were subsequently conducted using NSCLC cells cocultured with fibroblasts in the non-contact co-culture device. A schematic diagram of the device is shown in **Figure 4F**, and a modified version is shown in Supplementary Figure 1C. The AO/EB assay showed that neither the down-regulation of FUT8 in CAFs nor the up-regulation of FUT8 in HLFs could change NSCLC cell apoptosis in the co-culture system (Supplementary Figure 2A). This result was confirmed by Annexin V/propidium iodide (AV/PI) staining and flow cytometry apoptosis assays (Supplementary Figure 2B).

To investigate the effect of FUT8 in CAFs on the cell cycle progression of NSCLC cells, NSCLC cells cocultured with fibroblasts (CAFs-NC, CAFs-shFUT8, HLFs-FUT8 OE, and HLFs-NC) were subjected to PI staining and flow cytometry analysis. The results showed that the down-regulation of FUT8 in CAFs led to G1/S checkpoint blockage in the co-cultured NSCLC cells (**Figure 4G**). However, no change in the cell cycle in NSCLC cells was observed between the co-cultured with HLFs and HLF-FUT8 OE cells. The results indicated that FUT8/CF was necessary for CAFs to acquire the ability to promote cell cycle progression in NSCLC cells. However, the up-regulation of FUT8 alone in HLFs did not give the same ability to HLFs.

To explain these findings on proliferation, migration, invasion, and cell cycle regulation, we investigated several signaling pathways in A549 cells co-cultured with fibroblasts (CAFs-NC, CAFs-shFUT8, HLFs-FUT8 OE, and HLFs-NC) by western blot assays. The results showed that the down-regulation of FUT8 in CAFs led to inhibition of the MAPK/ERK1/2 pathway (**Figure 4H**) and to the expression of EMT (**Figure 4I**), and G1/S checkpoint (**Figure 4J**) biomarkers in NSCLC cells. However, the up-regulation of FUT8 in HLFs did not induce a corresponding increase in these signaling pathways in NSCLC cells.

Potential mechanisms through which FUT8 regulates the cancer-promoting phenotype of CAFs

To explain the potential mechanisms through which FUT8 contributes to the maintenance of the tumor-promoting phenotype of CAFs, the genome data from 15 CAF cell lines in the GSE22862 gene chip were analyzed by gene set enrichment analysis (GSEA). Four signaling pathways were found to be significantly enriched by the up-regulation and down-regulation of the FUT8 expression in CAFs. As shown by the gene enrichment indexes, the ErbB tyrosine kinase receptor family pathway, the apoptosis regulation network, and the β-alanine metabolism pathway were negatively enriched in FUT8 down-regulated CAFs (Supplementary Figure 3A-C), whereas the neuroactive ligand receptors pathway was positively enriched in FUT8 up-regulated CAFs (Supplementary Figure 3D).

In the current study, we focused on the finding that the ErbB pathway was blocked in CAFs with low FUT8 expression. To better describe the changes in the ErbB pathway, the mRNA expression levels of ErbB members and their down-stream genes are shown in a heatmap (**Figure 5A**). Heatmaps of the other three significantly enriched pathways are shown in the supplementary data (Supplementary Figure 3E-G). Further analysis showed that none of the ErbB genes (EGFR, HER2, HER3, and HER4) exhibited differential expression between CAFs with high and low FUT8 expression (**Figure 5B**). However, the mRNA expression of some signaling molecules downstream of ErbB1 (more commonly known as EGFR), such as PIK3CA (PI3Kp110α), PIK3CB (PI3Kp110β), PTEN,

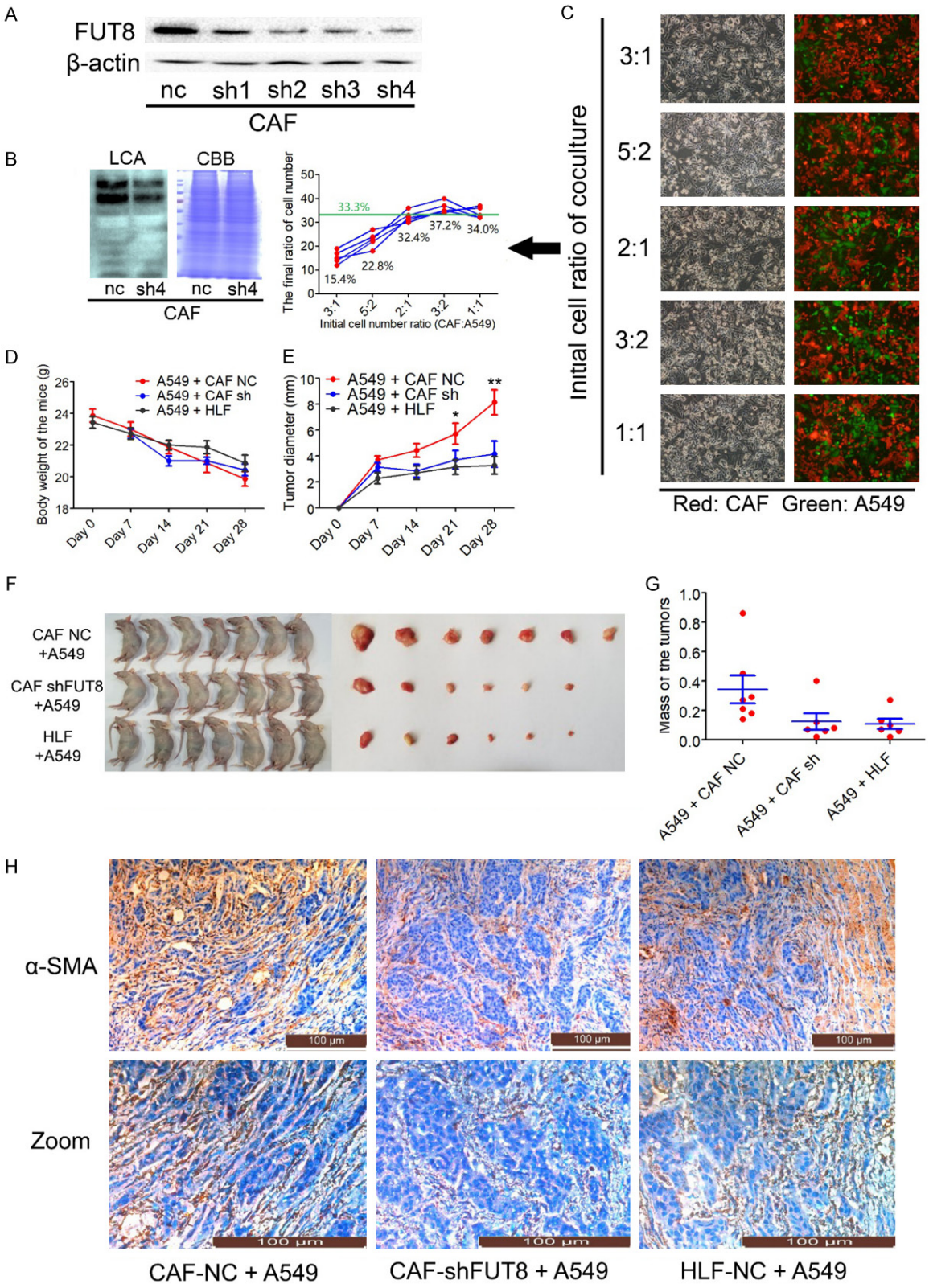

Figure 3. FUT8 in CAFs is necessary for the construction of an invasive TME in vivo. A. Four shRNA fragments were used to down-regulate FUT8 in CAFs, and the effects of this gene intervention were tested by western blotting. B. Lentivirus-packed sh4 was used to stably down-regulate FUT8 in CAFs, and the effect was tested by a lectin blot analysis. C. Fluorescently labeled A549 cells (green) and CAFs (red) were co-cultured continuously in vitro to inves-

tigate the appropriate ratio for co-injection. Magnification: 200×. Quantitative data are shown in the line chart on the right side. D. The changes in the body weights of the mice are shown in the line chart. E. The changes in the tumor diameters are shown in the line chart. F. Nude mice in the experiment and the generated tumors. G. The wet weights of the tumors removed from the mice are shown by the dot chart. H. Microstructures of the tumors generated by subcutaneous co-injection in nude mice. The tumor stroma was marked by IHC staining of α-SMA. Scale bar: 100 μm.

mTOR, STAT3, STAT5A, and STAT5B, was significantly down-regulated in CAFs with low FUT8 expression (**Figure 5C**).

CF mediated by FUT8 regulates the cancer-promoting capacity of CAFs by modifying EGFR fucosylation

To confirm the relationship between FUT8 expression and EGFR signaling, we detected EGFR, phosphorylated EGFR, and FUT8 expression in the five pairs of primary CAFs/NLFs by western blotting. The results showed that EGFR expression did not differ between CAFs and NLFs, whereas p-EGFR and FUT8 expression exhibited a consistent change (**Figure 6A**). To investigate whether the binding of fucose to EGFR protein was mediated by FUT8, EGFR was precipitated using immunomagnetic beads, and the level of fucose binding to EGFR was detected by lectin (LCA) blot assays. The results showed that the fucose modification of EGFR was consistent with the expression of FUT8 in both CAFs and HLFs (**Figure 6B**).

Subsequently, we investigated whether EGFR signaling exerts a promoting effect on the abilities of CAFs and whether EGFR signaling activity is regulated by FUT8/CF. First, we used four shRNA fragments to down-regulate EGFR expression in CAFs, and the effect of sh2 was the most significant (**Figure 6C**). Sh2 was used to stably down-regulate EGFR in CAFs and HLFs, and a subsequent clone formation assay showed that the down-regulation of either EGFR or FUT8 led to reduction in the cancer-promoting capacity of CAFs (**Figure 6D**). The up-regulation of FUT8 slightly enhanced the cancer-promoting capacity of HLFs, and down-regulation of EGFR in HLF-FUT8 OE cells counteracted this capacity (**Figure 6E**). Rescue experiments using CAFs and HLFs were conducted, and the results are shown in **Figure 6F**, **6G**. In CAFs, the down-regulation of either EGFR or FUT8 led to reduced phosphorylation of EGFR and its downstream molecules such as ERK, AKT, and JAK. However, the blocked EGFR signalings were rescued by treatment with an EGFR activator in FUT8 low-expressing CAFs. Similarly, in HLFs, the up-regulation of FUT8 led to increased phosphorylation of EGFR and its downstream molecules, and this effect was counteracted by EGFR-shRNA, and rescued again by treatment with an EGFR activator. The results strongly suggested that EGFR activity and its downstream signaling in CAFs were regulated by FUT8/CF modification and that EGFR signaling exerted a promoting effect on the cancer-promoting capacity of CAFs.

Discussion

In the current study, we explored the expression of FUT8 in CAFs through analyses of bioinformatics data and pathological tissues from NSCLC patients. We also demonstrated that FUT8-mediated CF exerted an effect on CAFs to promote an invasive TME in vivo, and in this environment, NSCLC cells showed faster growth and increased aggressiveness. Subsequently, we tested the promoting effect mediated by FUT8 on NSCLC with regard to tumor cell proliferation, apoptosis, cell cycle, migration, and invasion. In addition, we analyzed the potential mechanism through which FUT8 regulates CAFs in silico and predicted that the EGFR signaling pathway was regulated by FUT8. Additionally, we found that the FUT8-mediated activation of EGFR in CAFs exerted a promoting effect on NSCLC proliferation. A concise schematic diagram is shown in **Figure 7**, and this diagram should provide an easier understanding of the findings obtained in this study.

TME is the direct environment for the growth of tumor cells. In NSCLC, the TME is mainly composed of CAFs and immune cells, which play an important role in promoting a malignant environment for the development of NSCLC [48]. CAFs are activated in the interaction with tumor cells, during which a series of molecular changes occur in CAFs, resulting in phenotypic transformation of CAFs to acquire and maintain a cancer-promoting capacity [7]. Our previous study reported that FUT8/CF plays a role in the transformation of pericytes into myofibroblasts

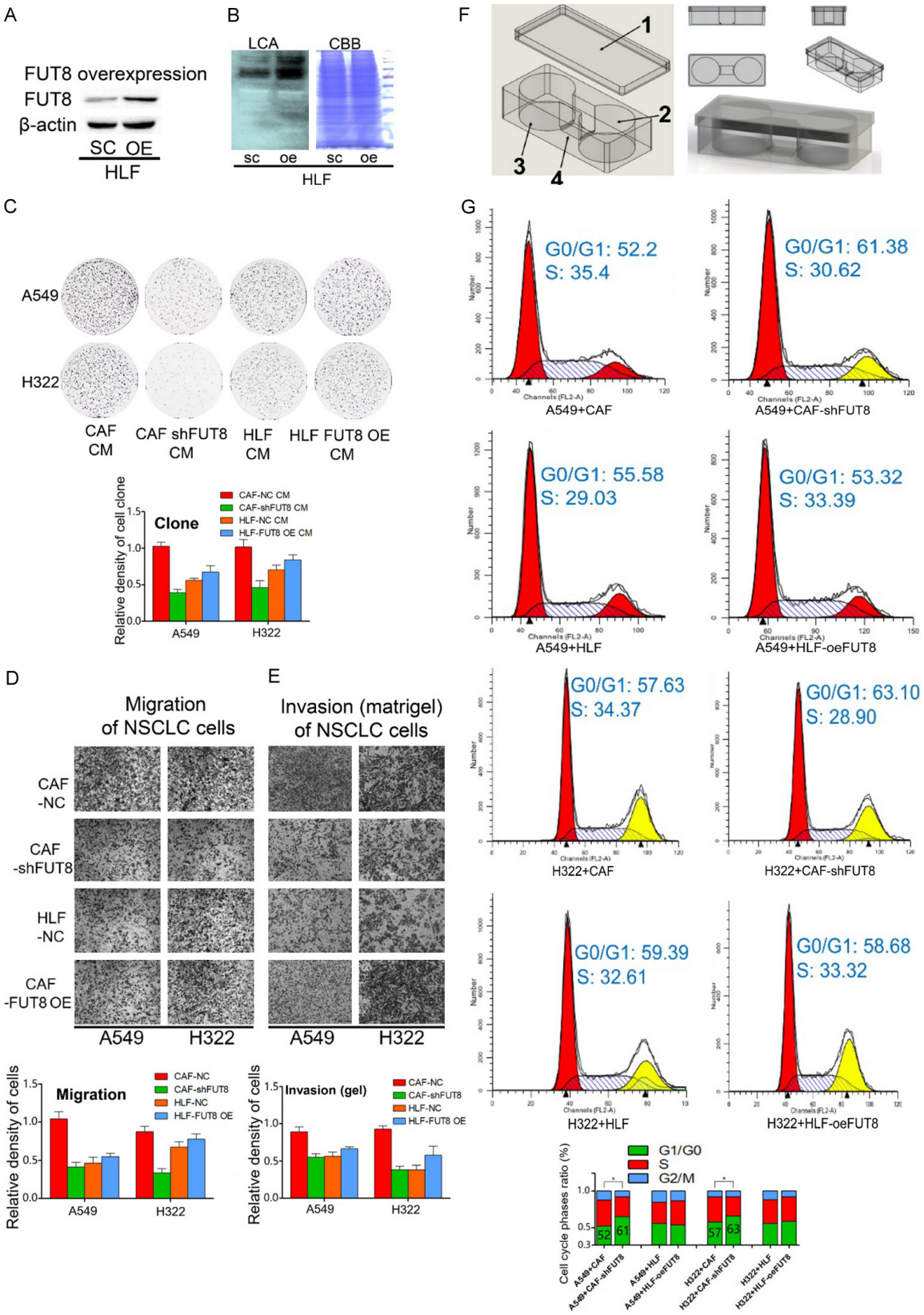
A
FUT8 overexpression
FUT8
β-actin
SC OE
HLF
B
LCA
CBB
sc oe sc oe
HLF
C
A549
H322
CAF CM
CAF shFUT8 CM
HLF CM
HLF FUT8 OE CM
Clone
CAF-NC CM
CAF-shFUT8 CM
HLF-NC CM
HLF-FUT8 OE CM
Relative density of cell clone
A549
H322
D
Migration of NSCLC cells
CAF -NC
CAF -shFUT8
HLF -NC
CAF -FUT8 OE
A549
H322
Migration
Relative density of cells
E
Invasion (matrigel) of NSCLC cells
Invasion (gel)
F
1
2
3
4
G
G0/G1: 52.2
S: 35.4
A549+CAF
G0/G1: 61.38
S: 30.62
A549+CAF-shFUT8
G0/G1: 55.58
S: 29.03
A549+HLF
G0/G1: 53.32
S: 33.39
A549+HLF-oeFUT8
G0/G1: 57.63
S: 34.37
H322+CAF
G0/G1: 63.10
S: 28.90
H322+CAF-shFUT8
G0/G1: 59.39
S: 32.61
H322+HLF
G0/G1: 58.68
S: 33.32
H322+HLF-oeFUT8
G1/G0
S
G2/M
Cell cycle phases ratio (%)
52
61
57
63
A549+CAF
A549+CAF-shFUT8
A549+HLF
A549+HLF-oeFUT8
H322+CAF
H322+CAF-shFUT8
H322+HLF
H322+HLF-oeFUT8

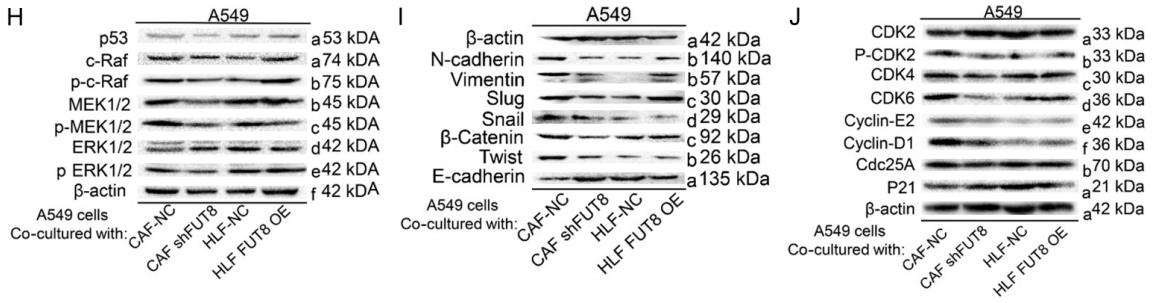

Figure 4. FUT8-mediated CF is necessary for the cancer-promoting capacity of CAFs. A. A lentivirus-packed FUT8 coding sequence was used to stably up-regulate FUT8 in HLFs. B. The effect of FUT8 up-regulation was tested by western blotting and lectin blotting analyses. C. The proliferation of A549 and H322 cells cultured with CM from CAFs or HLFs was tested by clone formation assays. D, E. A549 and H322 cells were co-cultured with fibroblasts in Transwell chambers, and the cell migration and invasion of NSCLC cells were tested. Magnification: 200×. F. Schematic diagram of the device used for the establishment of an in vitro non-contact co-culture system. A more detailed blueprint for 3D printing is available free from the corresponding authors upon request. 1: lid. 2: NSCLC cells. 3: CAFs/NLFs/HLFs. 4: precipitation well. G. The cell cycle of A549 and H322 cells co-cultured with fibroblasts was tested by PI staining and flow cytometry. Yellow peaks: diploids were observed in the assessed cells. H-J. A549 cells were co-cultured with fibroblasts in the non-contact co-culture system. The MAPK/ERK1/2 signaling pathway and biomarkers of EMT and the G1/S checkpoint in A549 cells were tested by western blot analysis. Protein bands with the same subscript letter were transferred from the same SDS-PAGE gel. All experiments were repeated three times.

[30]. Since the activation of CAFs was also characterized as a phenotypic transformation into myofibroblasts, we assumed that FUT8/CF also plays a promoting role in CAFs. Some researchers have reported that FUT8 was active in cancer. In addition to its high expression in malignant tumors and its role as a prognostic factor [16], FUT8 is also involved in regulating the activity of cancer-associated molecules, such as EGFR [17], p53 [49], E-cadherin [50], and L1 cell adhesion molecule (L1CAM) [51]. However, the current study is the first to report the role of FUT8 in the TME.

A novel finding of this study was that FUT8 was overexpressed in not only NSCLC cells but also the tumor stroma of six out of eight cases. To better study the effect of FUT8 in CAFs, we isolated CAFs and NLFs from 5 out of 10 NSCLC patients, but we failed to isolate paired fibroblasts from the other five patients (case P02, P04, P05, P09, and P10) due to the difficulty associated with the in vitro culture of NLFs. We then identified the primary CAFs with myofibroblast markers. Although some previous reports have indicated the existence of morphological differences between CAFs and NLFs [52-54], no significant differences were observed in the current study. Next, we found that FUT8 and CF were overexpressed in the primary CAFs from three out of five cases. However, primary NLFs grew very slowly in the co-culture system. The growth of NLFs almost stopped after eight to ten passages, even though they were immortalized. Therefore, we selected lab-grown HLFs as controls for CAFs in subsequent experiments.

In the current study, fibroblasts were co-cultured with NSCLC cells. Previous researchers have used many methods for the in vitro and in vivo stimulation of the TME, particularly for restoring the interaction between CAFs and tumor cells. The classic models include CM, the Transwell system [55], the Boyden chamber system [56], and xenoanimal co-injection models [57]. In recent years, microfluidic chip technology [58] and the patient-derived xenograft mouse models (PDXs) [59] have also become common research tools. In the current study, we introduced a novel noncontact co-culture device that overcomes the limitations of previous methods associated with the cell quantity and the need for continuous passage. The application of this new device ensured that some cell experiments could be performed directly under non-contact co-culture conditions and that sufficient cells can be harvested for further analysis.

The most important phenomenon of this study was obtained from the subcutaneous co-injection tumorigenesis assays using nude mice. In primary NSCLC, CAFs account for 70% of the cells in solid tumors. This ratio of cell compo-

A

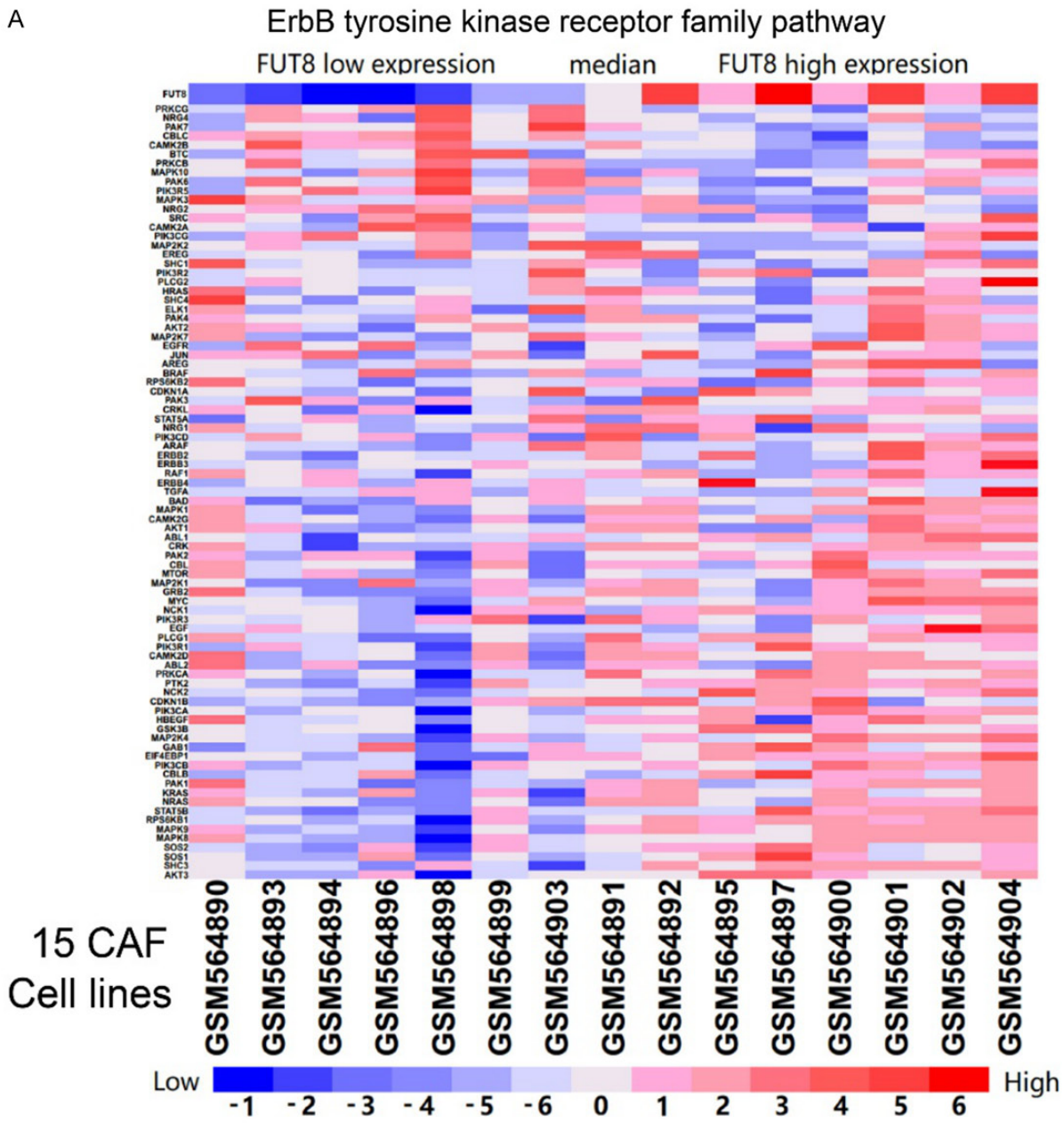
ErbB tyrosine kinase receptor family pathway
FUT8 low expression
median
FUT8 high expression
FUT8
PRKCG
NRG4
PAK7
CBLC
CAMK2B
BTC
PRKCB
MAPK10
PAK6
PIK3R5
MAPK3
NRG2
SRC
CAMK2A
PIK3CG
MAP2K2
EREG
SHC1
PIK3R2
PLCG2
HRAS
SHC4
ELK1
PAK4
AKT2
MAP2K7
EGFR
JUN
AREG
BRAF
RPS6KB2
CDKN1A
PAK3
CRKL
STAT5A
NRG1
PIK3CD
ARAF
ERBB2
ERBB3
RAF1
ERBB4
TGFA
BAD
MAPK1
CAMK2G
AKT1
ABL1
CRK
PAK2
CBL
MTOR
MAP2K1
GRB2
MYC
NCK1
PIK3R3
EGF
PLCG1
PIK3R1
CAMK2D
ABL2
PRKCA
PTK2
NCK2
CDKN1B
PIK3CA
HBEGF
GSK3B
MAP2K4
GAB1
EIF4EBP1
PIK3CB
CBLB
PAK1
KRAS
NRAS
STAT5B
RPS6KB1
MAPK9
MAPK8
SOS2
SOS1
SHC3
AKT3
15 CAF
Cell lines
GSM564890
GSM564893
GSM564894
GSM564896
GSM564898
GSM564899
GSM564903
GSM564891
GSM564892
GSM564895
GSM564897
GSM564900
GSM564901
GSM564902
GSM564904
Low
High
-1
-2
-3
-4
-5
-6
0
1
2
3
4
5
6

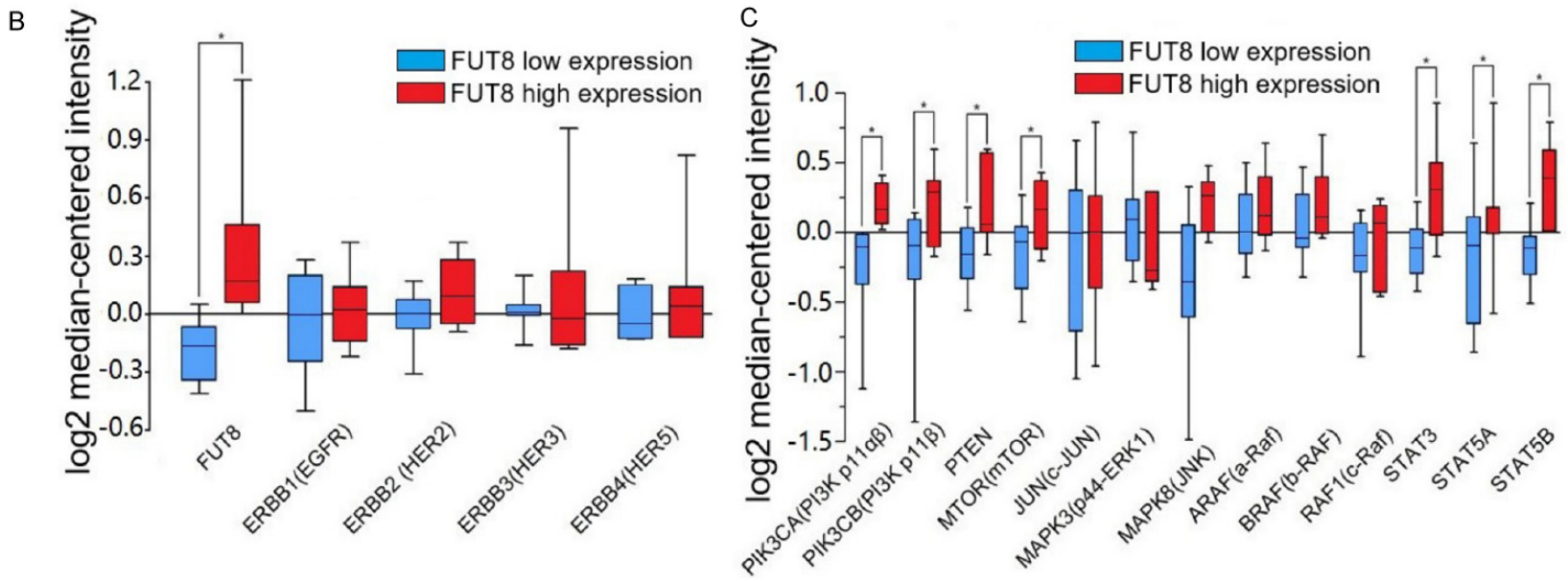

Figure 5. Potential mechanisms through which FUT8 regulates the cancer-promoting phenotype of CAFs. A. Heatmap based on the expression of genes in the ErbB family pathway. The colors represent normalized z-scores to illustrate the relative values within rows and cannot be used to compare values between rows. B. The expression of the ErbB genes in the FUT8 high/low groups. C. The expression of genes downstream of EGFR in the groups with high and low FUT8 expression. Raw GSEA data are available from the corresponding authors upon request.

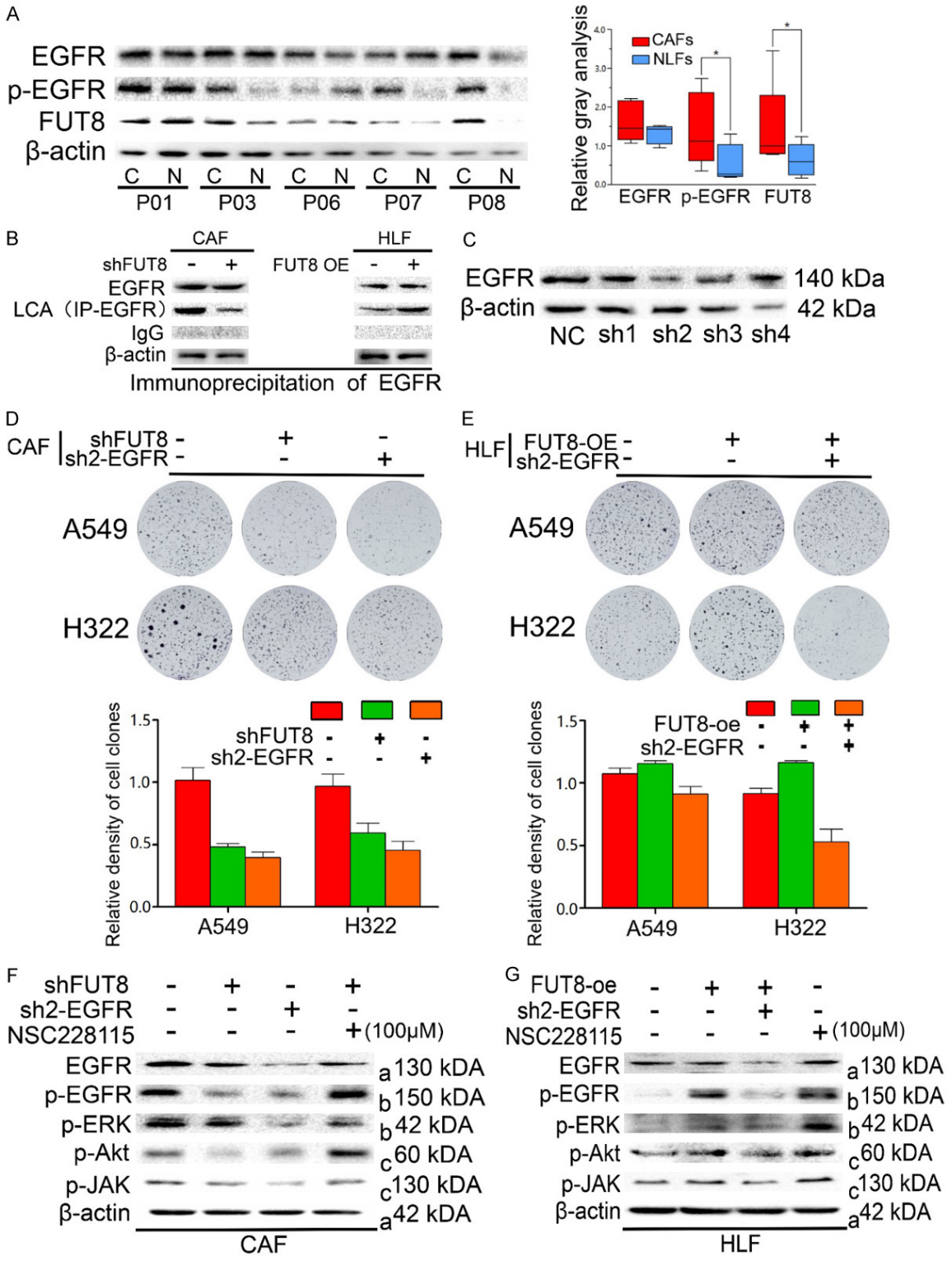

Figure 6. CF mediated by FUT8 regulates the cancer-promoting capacity of CAFs via the modification of EGFR fucosylation. A. The expression of EGFR, p-EGFR, and FUT8 in primary CAFs and paired NLFs were tested by western blot analysis. C: CAFs. N: NLFs. B. The binding of fucose to EGFR was tested by immunoprecipitation (IP) and a lectin blot. C. Four shRNA fragments were used for the knockdown of FUT8 in CAFs, and the effect was tested by western blotting. D. A549 and H322 cells were cultured with CM from CAFs. The proliferation of NSCLC cells was tested by a clone formation assay. E. A549 and H322 cells were cultured with CM from CAFs/HLFs. The proliferation of NSCLC cells was tested by a clone formation assay. F, G. EGFR signaling and the phosphorylation levels of ERK, JAK, and Akt

in CAFs or HLFs were tested by western blotting. NSC 228155 is an activator of EGFR that binds to the extracellular region of EGFR and enhances tyrosine phosphorylation of EGFR. Protein bands with the same subscript letter were transferred from the same SDS-PAGE gel. All experiments were repeated three times.

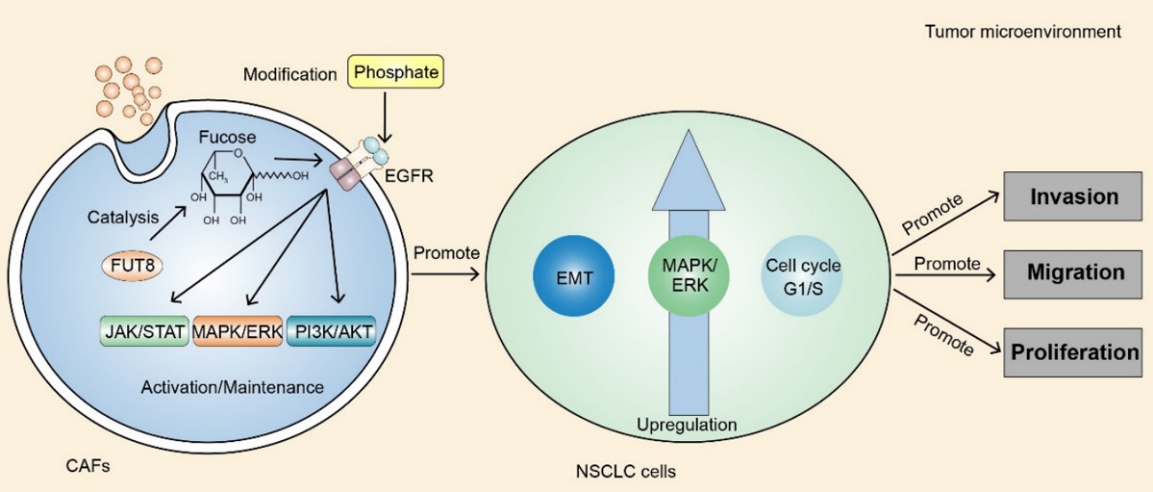

Figure 7. A concise schematic diagram of the mechanism elucidated in the current study.

nents allows the tumor to grow rapidly and steadily [5]. In our previous attempts, inappropriate co-injection ratios often resulted in imbalance of the two cell components. The majority of the cells gradually occupied the living space of the minority, which finally led to the failure of mimicking a TME. Thus, it was necessary to investigate a proper ratio for the cell mixture in an in vitro co-culture assay. We emphasized this preliminary experiment in the results section, rather than including it in the supplementary materials, because this experimental data were critical for successful tumorigenesis. The CAFs-NC/A549 cell mixture showed markedly increased tumor formation and growth abilities compared with the CAF-shFUT8/A549 and HLF-NC/A549 cell mixtures. IHC staining showed that CAF-NC/A549 cells generated a very invasive TME. In contrast, the CAF-shFU8/A549 tumors exhibited an inactive microenvironment in which the NSCLC cells rarely invaded into the stroma and compacted themselves into clumps.

To explain the effect of FUT8/CF in CAFs on tumor proliferation and invasion, we investigated the mechanism through which FUT8/CF in CAFs acts on NSCLC cells in vitro. The results showed that the down-regulation of FUT8 in CAFs inhibited the proliferation of NSCLC cells. The down-regulation of FUT8 in CAFs prevented NSCLC cells from entering the G1/S phase. We also demonstrated the effects of FUT8/CF in CAFs on tumor migration and invasion. These malignant behaviors are closely associated with tumor proliferation and metastasis, which indicates that the down-regulation of FUT8/CF in CAFs led to inhibition of their tumor proliferation and metastasis abilities. However, these results implied that although FUT8 exerted a promoting effect on CAFs, the up-regulation of FUT8 alone did not confer the same capacity on HLFs.

To further explore the mechanism, a bioinformatics analysis was conducted. A GSEA showed that low FUT8/CF expression in CAFs led to inhibition of the ErbB pathway. We speculated that this effect is an important factor for the resulting inhibition of reason that inhibited the cancer-promoting capacity of CAFs with low FUT8 expression. The unchanged gene copy numbers of ErbB genes implied that the activities of these genes were regulated at neither the transcriptional nor translational level. Because previous studies revealed that EGFR (ErbB1) can only function if it is properly glycosylated [22, 60], we hypothesized that the down-regulation of FUT8 blocked the CF of EGFR and subsequently inhibited its downstream pathways.

Subsequently, we verified that EGFR activity in CAFs was regulated by FUT8/CF. We detected

the expression of EGFR and phosphorylated (activated) EGFR in CAFs and NLFs. The consistency of EGFR phosphorylation and FUT8 expression indicated that FUT8 exerted a promoting effect on EGFR phosphorylation. Next, the results from the immunoprecipitation and lection blot assays showed that the up-regulation/down-regulation of FUT8 induced changes in the levels of fucose binding to EGFR, which suggested that the CF modification of EGFR was regulated by FUT8. Moreover, the down-regulation of either FUT8 or EGFR in CAFs led to an inhibited ability to promote NSCLC cell proliferation, and the down-regulation of EGFR counteracted this ability in FUT8-overexpressing HLFs. ERK, AKT, and JAK are the key signaling molecules of the MAPK/ERK, PI3K/AKT/mTOR, and JAK/STAT signaling pathways, and are activated by phosphorylation. Finally, the results from rescue experiments suggested that the phosphorylation of EGFR, ERK, AKT, and JAK was regulated by FUT8 expression in CAFs and HLFs. Moreover, the regulation of ERK, AKT, and JAK phosphorylation by FUT8 occurred via the phosphorylation of EGFR. This result was in accordance with a previous finding that EGFR and its downstream signalings are relevant to the cancer-promoting capacity of CAFs in breast cancer [23]. Together, the results obtained in the current study support a novel conclusion regarding the function of FUT8 in CAFs of NSCLC.

In conclusion, FUT8-mediated CF in CAFs plays a positive role in the cancer-promoting capacity of CAFs. FUT8 overexpression was observed in CAFs of some lung adenocarcinoma cases. FUT8/CF in CAFs promoted the formation of an invasive and malignant TME in vivo and in vitro, and in this environment, NSCLC cells showed faster cell proliferation and greater invasiveness. EGFR signaling exerted a catalytic effect on the cancer-promoting capacity of CAFs and was regulated by the CF modification of the EGFR protein.

Our findings indicate that FUT8 and CF are potential candidates for studies on the formation and maintenance of TME. Besides, FUT8 is a potential therapeutic target for NSCLC. One limitation of the present study is that the molecular mechanism of FUT8 regulating EGFR signaling in CAFs was not thoroughly studied. In addition, we speculate that EGFR is probably not the only protein regulated by FUT8 in CAFs since CF is a crucial modification of many proteins. Further study is warranted to explore the mechanism of FUT8 regulating TME components.

Acknowledgements

We would like to acknowledge our colleagues from the Institute of Cancer Stem Cells of Dalian Medical University, and the Center for Kidney Diseases Translational Medicine of Liaoning Province. This work was supported by grants from the National Natural Science Foundation of China (81670063, 81774078 and 81774078).

Disclosure of conflict of interest

None.

Address correspondence to: Drs. Taihua Wu and Chundong Gu, The First Affiliated Hospital of Dalian Medical University, Zhongshan Road #222, Dalian 116000, Liaoning, China. Tel: +86 0411-83635963; E-mail: wutaihua@dmu.edu.cn (THW); guchundong@dmu.edu.cn (CDG)

References

[1] Siegel RL, Miller KD and Jemal A. Cancer statistics, 2018. CA Cancer J Clin 2018; 68: 7-30.

[2] Li F, Zhang S, Zhang Q, Li J, Zhao S and Gu C. CYP1B1 G199T polymorphism affects prognosis of NSCLC patients with the potential to be an indicator and target for precise drug intervention. Biomed Res Int 2017; 2017: 1529564.

[3] Ben Amar J, Ben Safta B, Zaibi H, Dhahri B, Baccar MA and Azzabi S. Prognostic factors of advanced stage non-small-cell lung cancer. Tunis Med 2016; 94: 360-367.

[4] Huang Y, Lin D and Taniguchi CM. Hypoxia inducible factor (HIF) in the tumor microenvironment: friend or foe. Sci China Life Sci 2017; 60: 1114-1124.

[5] Vicent S, Sayles LC, Vaka D, Khatri P, Gevaert O, Chen R, Zheng Y, Gillespie AK, Clarke N, Xu Y, Shrager J, Hoang CD, Plevritis S, Butte AJ and Sweet-Cordero EA. Cross-species functional analysis of cancer-associated fibroblasts identifies a critical role for CLCF1 and IL-6 in non-small cell lung cancer in vivo. Cancer Res 2012; 72: 5744-5756.

[6] Goicoechea SM, García-Mata R, Staub J, Valdivia A, Sharek L, McCulloch CG, Hwang RF, Urrutia R, Yeh JJ, Kim HJ and Otey CA. Palladin promotes invasion of pancreatic cancer cells

by enhancing invadopodia formation in cancer-associated fibroblasts. Oncogene 2014; 33: 1265-1273.
[7] Liao Z, Tan ZW, Zhu P and Tan NS. Cancer-associated fibroblasts in tumor microenvironment - Accomplices in tumor malignancy. Cell Immunol 2019; 343: 103729.
[8] Son B, Lee S, Youn H, Kim E, Kim W and Youn B. The role of tumor microenvironment in therapeutic resistance. Oncotarget 2017; 8: 3933-3945.
[9] Wang Y, Fukuda T, Isaji T, Lu J, Im S, Hang Q, Gu W, Hou S, Ohtsubo K and Gu J. Loss of α1,6-fucosyltransferase inhibits chemical-induced hepatocellular carcinoma and tumorigenesis by down-regulating several cell signaling pathways. FASEB J 2015; 29: 3217-3227.
[10] Cheng L, Luo S, Jin C, Ma H, Zhou H and Jia L. FUT family mediates the multidrug resistance of human hepatocellular carcinoma via the PI3K/Akt signaling pathway. Cell Death Dis 2013; 4: e923.
[11] Yang Q and Wang LX. Mammalian α-1,6-Fucosyltransferase (FUT8) Is the Sole Enzyme Responsible for the N-Acetylglucosaminyltransferase I-independent Core Fucosylation of High-mannose N-Glycans. J Biol Chem 2016; 291: 11064-11071.
[12] Honma R, Kinoshita I, Miyoshi E, Tomaru U, Matsuno Y, Shimizu Y, Takeuchi S, Kobayashi Y, Kaga K, Taniguchi N and Dosaka-Akita H. Expression of fucosyltransferase 8 is associated with an unfavorable clinical outcome in non-small cell lung cancers. Oncology 2015; 88: 298-308.
[13] Tu CF, Wu MY, Lin YC, Kannagi R and Yang RB. FUT8 promotes breast cancer cell invasiveness by remodeling TGF-β receptor core fucosylation. Breast Cancer Res 2017; 19: 111.
[14] Yue L, Han C, Li Z, Li X, Liu D, Liu S and Yu H. Fucosyltransferase 8 expression in breast cancer patients: a high throughput tissue microarray analysis. Histol Histopathol 2016; 31: 547-555.
[15] Hu P, Shi B, Geng F, Zhang C, Wu W and Wu XZ. E-cadherin core fucosylation regulates nuclear beta-catenin accumulation in lung cancer cells. Glycoconj J 2008; 25: 843-850.
[16] Kossowska B, Ferens-Sieczkowska M, Gancarz R, Passowicz-Muszyńska E and Jankowska R. Fucosylation of serum glycoproteins in lung cancer patients. Clin Chem Lab Med 2005; 43: 361-369.
[17] Liu YC, Yen HY, Chen CY, Chen CH, Cheng PF, Juan YH, Chen CH, Khoo KH, Yu CJ, Yang PC, Hsu TL and Wong CH. Sialylation and fucosylation of epidermal growth factor receptor suppress its dimerization and activation in lung cancer cells. Proc Natl Acad Sci U S A 2011; 108: 11332-11337.
[18] Gandhi J, Zhang J, Xie Y, Soh J, Shigematsu H, Zhang W, Yamamoto H, Peyton M, Girard L, Lockwood WW, Lam WL, Varella-Garcia M, Minna JD and Gazdar AF. Alterations in genes of the EGFR signaling pathway and their relationship to EGFR tyrosine kinase inhibitor sensitivity in lung cancer cell lines. PLoS One 2009; 4: e4576.
[19] Andersson U, Schwartzbaum J, Wiklund F, Sjöström S, Liu Y, Tsavachidis S, Ahlbom A, Auvinen A, Collatz-Laier H, Feychting M, Johansen C, Kiuru A, Lönn S, Schoemaker MJ, Swerdlow AJ, Henriksson R, Bondy M and Melin B. A comprehensive study of the association between the EGFR and ERBB2 genes and glioma risk. Acta Oncol 2010; 49: 767-775.
[20] Norman J, Badie-Dezfooly B, Nord EP, Kurtz I, Schlosser J, Chaudhari A and Fine LG. EGF-induced mitogenesis in proximal tubular cells: potentiation by angiotensin II. Am J Physiol 1987; 253: F299-309.
[21] Matsumoto K, Yokote H, Arao T, Maegawa M, Tanaka K, Fujita Y, Shimizu C, Hanafusa T, Fujiwara Y and Nishio K. N-Glycan fucosylation of epidermal growth factor receptor modulates receptor activity and sensitivity to epidermal growth factor receptor tyrosine kinase inhibitor. Cancer Sci 2008; 99: 1611-1617.
[22] Wang X, Gu J, Ihara H, Miyoshi E, Honke K and Taniguchi N. Core fucosylation regulates epidermal growth factor receptor-mediated intracellular signaling. J Biol Chem 2006; 281: 2572-2577.
[23] Pisano A, Santolla MF, De Francesco EM, De Marco P, Rigiracciolo DC, Perri MG, Vivacqua A, Abonante S, Cappello AR, Dolce V, Belfiore A, Maggiolini M and Lappano R. GPER, IGF-IR, and EGFR transduction signaling are involved in stimulatory effects of zinc in breast cancer cells and cancer-associated fibroblasts. Mol Carcinog 2017; 56: 580-593.
[24] Luo H, Yang G, Yu T, Luo S, Wu C, Sun Y, Liu M and Tu G. GPER-mediated proliferation and estradiol production in breast cancer-associated fibroblasts. Endocr Relat Cancer 2014; 21: 355-369.
[25] Álvarez-Teijeiro S, García-Inclán C, Villaronga MÁ, Casado P, Hermida-Prado F, Granda-Díaz R, Rodrigo JP, Calvo F, Del-Río-Ibisate N, Gandarillas A, Morís F, Hermsen M, Cutillas P and García-Pedrero JM. Factors secreted by cancer-associated fibroblasts that sustain cancer stem properties in head and neck squamous carcinoma cells as potential therapeutic targets. Cancers (Basel) 2018; 10.
[26] Suzuki E, Yamazaki S, Naito T, Hashimoto H, Okubo S, Udagawa H, Goto K, Tsuboi M, Ochiai A and Ishii G. Secretion of high amounts of hepatocyte growth factor is a characteristic fea-

ture of cancer-associated fibroblasts with EGFR-TKI resistance-promoting phenotype-A study of 18 cases of cancer-associated fibroblasts. Pathol Int 2019; 69: 472-480.
[27] Yi Y, Zeng S, Wang Z, Wu M, Ma Y, Ye X, Zhang B and Liu H. Cancer-associated fibroblasts promote epithelial-mesenchymal transition and EGFR-TKI resistance of non-small cell lung cancers via HGF/IGF-1/ANXA2 signaling. Biochim Biophys Acta Mol Basis Dis 2018; 1864: 793-803.
[28] Gao MQ, Kim BG, Kang S, Choi YP, Yoon JH and Cho NH. Human breast cancer-associated fibroblasts enhance cancer cell proliferation through increased TGF-α cleavage by ADAM17. Cancer Lett 2013; 336: 240-246.
[29] Han ME, Kim HJ, Shin DH, Hwang SH, Kang CD and Oh SO. Overexpression of NRG1 promotes progression of gastric cancer by regulating the self-renewal of cancer stem cells. J Gastroenterol 2015; 50: 645-656.
[30] Sun W, Tang H, Gao L, Sun X, Liu J, Wang W, Wu T and Lin H. Mechanisms of pulmonary fibrosis induced by core fucosylation in pericytes. Int J Biochem Cell Biol 2017; 88: 44-54.
[31] Hou GX, Liu P, Yang J and Wen S. Mining expression and prognosis of topoisomerase isoforms in non-small-cell lung cancer by using Oncomine and Kaplan-Meier plotter. PLoS One 2017; 12: e0174515.
[32] Liu W, Ouyang S, Zhou Z, Wang M, Wang T, Qi Y, Zhao C, Chen K and Dai L. Identification of genes associated with cancer progression and prognosis in lung adenocarcinoma: analyses based on microarray from oncomine and the cancer genome atlas databases. Mol Genet Genomic Med 2019; 7: e00528.
[33] Xu B, Liu N, Chen SQ, Jiang H, Zhang LJ, Zhang XW, Yang Y, Sha GZ, Liu J, Zhu WD and Chen M. Expression of SRD5A1 and its prognostic role in prostate cancer: analysis based on the data-mining of ONCOMINE. Zhonghua Nan Ke Xue 2016; 22: 771-776.
[34] Asamura H, Chansky K, Crowley J, Goldstraw P, Rusch VW, Vansteenkiste JF, Watanabe H, Wu YL, Zielinski M, Ball D and Rami-Porta R. The international association for the study of lung cancer lung cancer staging project: proposals for the revision of the N descriptors in the forthcoming 8th edition of the TNM classification for lung cancer. J Thorac Oncol 2015; 10: 1675-1684.
[35] Zhao S, Guo W, Li J, Yu W, Guo T, Deng W and Gu C. High expression of Y-box-binding protein 1 correlates with poor prognosis and early recurrence in patients with small invasive lung adenocarcinoma. Onco Targets Ther 2016; 9: 2683-2692.
[36] Zhao S, Guo T, Li J, Uramoto H, Guan H, Deng W and Gu C. Expression and prognostic value of GalNAc-T3 in patients with completely resected small (≤2 cm) peripheral lung adenocarcinoma after IASLC/ATS/ERS classification. Onco Targets Ther 2015; 8: 3143-3152.
[37] Travis WD, Brambilla E, Burke AP, Marx A and Nicholson AG. Introduction to the 2015 world health organization classification of tumors of the lung, pleura, thymus, and heart. J Thorac Oncol 2015; 10: 1240-1242.
[38] Travis WD, Brambilla E, Noguchi M, Nicholson AG, Geisinger KR, Yatabe Y, Beer DG, Powell CA, Riely GJ, Van Schil PE, Garg K, Austin JH, Asamura H, Rusch VW, Hirsch FR, Scagliotti G, Mitsudomi T, Huber RM, Ishikawa Y, Jett J, Sanchez-Cespedes M, Sculier JP, Takahashi T, Tsuboi M, Vansteenkiste J, Wistuba I, Yang PC, Aberle D, Brambilla C, Flieder D, Franklin W, Gazdar A, Gould M, Hasleton P, Henderson D, Johnson B, Johnson D, Kerr K, Kuriyama K, Lee JS, Miller VA, Petersen I, Roggli V, Rosell R, Saijo N, Thunnissen E, Tsao M and Yankelewitz D. International association for the study of lung cancer/american thoracic society/european respiratory society international multidisciplinary classification of lung adenocarcinoma. J Thorac Oncol 2011; 6: 244-285.
[39] Liu L, Liu L, Yao HH, Zhu ZQ, Ning ZL and Huang Q. Stromal myofibroblasts are associated with poor prognosis in solid cancers: a meta-analysis of published studies. PLoS One 2016; 11: e0159947.
[40] Kilvaer TK, Khanehkenari MR, Hellevik T, Al-Saad S, Paulsen EE, Bremnes RM, Busund LT, Donnem T and Martinez IZ. Cancer associated fibroblasts in stage I-IIIA NSCLC: prognostic impact and their correlations with tumor molecular markers. PLoS One 2015; 10: e0134965.
[41] Tsujino T, Seshimo I, Yamamoto H, Ngan CY, Ezumi K, Takemasa I, Ikeda M, Sekimoto M, Matsuura N and Monden M. Stromal myofibroblasts predict disease recurrence for colorectal cancer. Clin Cancer Res 2007; 13: 2082-2090.
[42] Yamashita M, Ogawa T, Zhang X, Hanamura N, Kashikura Y, Takamura M, Yoneda M and Shiraishi T. Role of stromal myofibroblasts in invasive breast cancer: stromal expression of alpha-smooth muscle actin correlates with worse clinical outcome. Breast Cancer 2012; 19: 170-176.
[43] Inoue C, Tamatsuki D, Miki Y, Saito R, Okada Y and Sasano H. Prognostic significance of combining immunohistochemical markers for cancer-associated fibroblasts in lung adenocarcinoma tissue. Virchows Arch 2019; 475: 181-189.
[44] Li F, Zhao S, Guo T, Li J and Gu C. The nutritional cytokine leptin promotes NSCLC by activating the PI3K/AKT and MAPK/ERK pathways in NSCLC cells in a paracrine manner. Biomed Res Int 2019; 2019: 2585743.

[45] Zhao S, Wang Y, Guo T, Yu W, Li J, Tang Z, Yu Z, Zhao L, Zhang Y, Wang Z, Wang P, Li Y, Li F, Sun Z, Xuan Y, Tang R, Deng WG, Guo W and Gu C. YBX1 regulates tumor growth via CDC25a pathway in human lung adenocarcinoma. Oncotarget 2016; 7: 82139-82157.

[46] Guo T, Zhao S, Wang P, Xue X, Zhang Y, Yang M, Li N, Li Z, Xu L, Jiang L, Zhao L, Ma PC, Rosell R, Li J and Gu C. YB-1 regulates tumor growth by promoting MACC1/c-Met pathway in human lung adenocarcinoma. Oncotarget 2017; 8: 48110-48125.

[47] Rio DC, Ares M, Hannon GJ and Nilsen TW. Purification of RNA using TRIzol (TRI reagent). Cold Spring Harb Protoc 2010; 2010: pdb.prot5439.

[48] Wood SL, Pernemalm M, Crosbie PA and Whetton AD. The role of the tumor-microenvironment in lung cancer-metastasis and its relationship to potential therapeutic targets. Cancer Treat Rev 2014; 40: 558-566.

[49] Sasaki H, Toda T, Furukawa T, Mawatari Y, Takaesu R, Shimizu M, Wada R, Kato D, Utsugi T, Ohtsu M and Murakami Y. α-1,6-Fucosyltransferase (FUT8) inhibits hemoglobin production during differentiation of murine and K562 human erythroleukemia cells. J Biol Chem 2013; 288: 16839-16847.

[50] Shao K, Chen ZY, Gautam S, Deng NH, Zhou Y and Wu XZ. Posttranslational modification of E-cadherin by core fucosylation regulates Src activation and induces epithelial-mesenchymal transition-like process in lung cancer cells. Glycobiology 2016; 26: 142-154.

[51] Agrawal P, Fontanals-Cirera B, Sokolova E, Jacob S, Vaiana CA, Argibay D, Davalos V, McDermott M, Nayak S, Darvishian F, Castillo M, Ueberheide B, Osman I, Fenyö D, Mahal LK and Hernando E. A systems biology approach identifies FUT8 as a driver of melanoma metastasis. Cancer Cell 2017; 31: 804-819, e7.

[52] 16.8.12 Clonal heterogeneity in osteogenic potential of lung cancer associated fibroblasts [PMIDZ27119516]. 2016.

[53] Horie M, Saito A, Mikami Y, Ohshima M, Morishita Y, Nakajima J, Kohyama T and Nagase T. 16.8.10 Characterization of human lung cancer-associated fibroblasts in three-dimensional in vitro co-culture model. Biochem Biophys Res Commun 2012; 423: 158-163.

[54] Kim SH, Choe C, Shin YS, Jeon MJ, Choi SJ, Lee J, Bae GY, Cha HJ and Kim J. Human lung cancer-associated fibroblasts enhance motility of non-small cell lung cancer cells in co-culture. Anticancer Res 2013; 33: 2001-2009.

[55] Lv G, Tan Y, Lv H, Fang T, Wang C, Li T, Yu Y, Hu C, Wen W, Wang H and Yang W. MXR7 facilitates liver cancer metastasis via epithelial-mesenchymal transition. Sci China Life Sci 2017; 60: 1203-1213.

[56] Hebeiss I, Truckenmüller R, Giselbrecht S and Schepers U. Novel three-dimensional Boyden chamber system for studying transendothelial transport. Lab Chip 2012; 12: 829-834.

[57] Olumi AF, Grossfeld GD, Hayward SW, Carroll PR, Tlsty TD and Cunha GR. Carcinoma-associated fibroblasts direct tumor progression of initiated human prostatic epithelium. Cancer Res 1999; 59: 5002-5011.

[58] Zhang Q, Liu T and Qin J. A microfluidic-based device for study of transendothelial invasion of tumor aggregates in realtime. Lab Chip 2012; 12: 2837-2842.

[59] Igarashi K, Murakami T, Kawaguchi K, Kiyuna T, Miyake K, Zhang Y, Nelson SD, Dry SM, Li Y, Yanagawa J, Russell TA, Singh AS, Tsuchiya H, Elliott I, Eilber FC and Hoffman RM. A patient-derived orthotopic xenograft (PDOX) mouse model of a cisplatinum-resistant osteosarcoma lung metastasis that was sensitive to temozolomide and trabectedin: implications for precision oncology. Oncotarget 2017; 8: 62111-62119.

[60] Azimzadeh Irani M, Kannan S and Verma C. Role of N-glycosylation in EGFR ectodomain ligand binding. Proteins 2017; 85: 1529-1549.

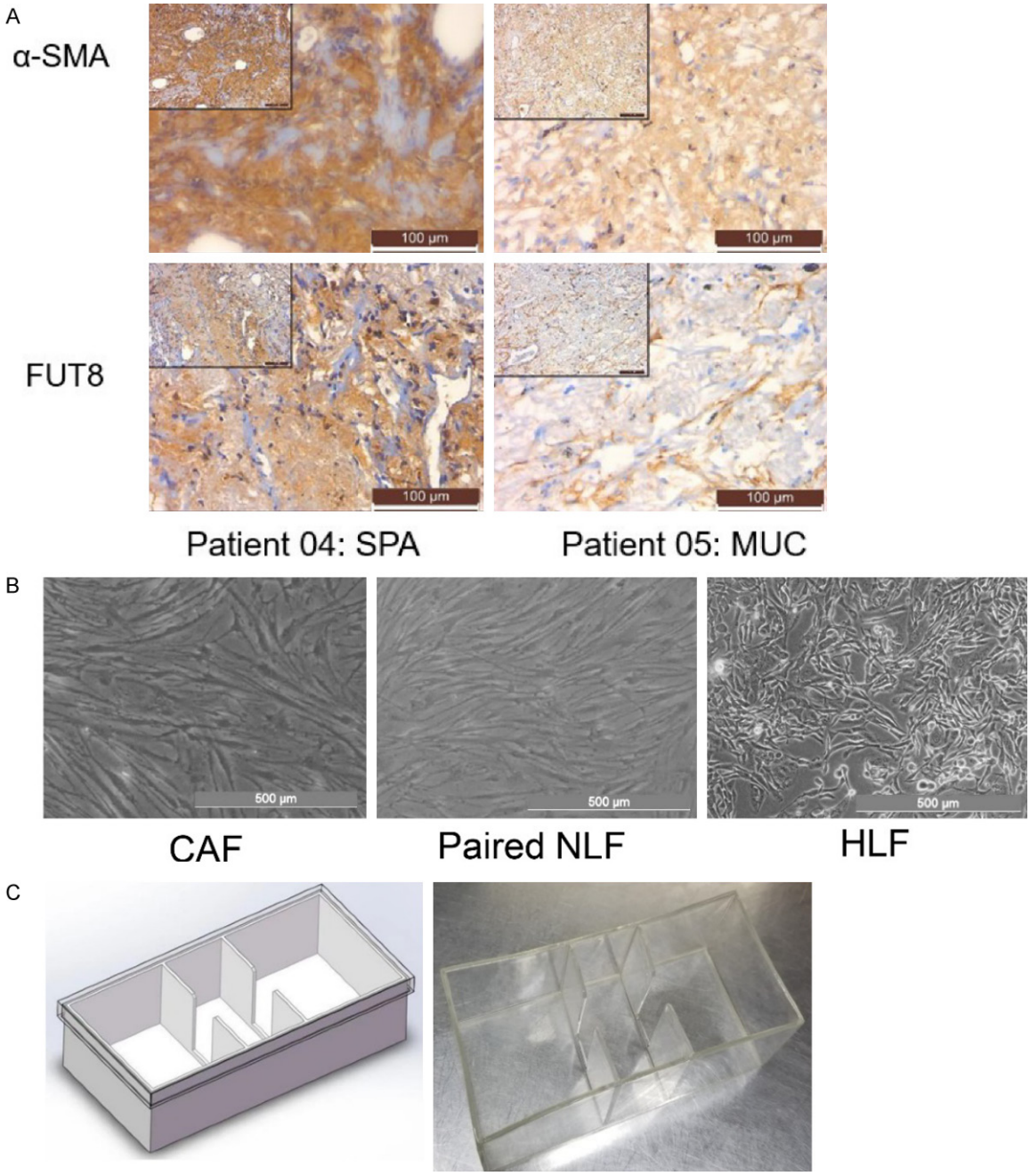

Supplementary Figure 1. A. Representative images of IHC staining of α-SMA and FUT8 in the two excluded histological subtypes of lung adenocarcinoma. SPA: solid predominant adenocarcinoma, MUC: mucinous adenocarcinoma. B. Morphological characteristics were observed under a microscope. Scale bar: 500 μm. C. Schematic diagram and real photograph of the improved design of the co-culture device used in the current study. A more detailed blueprint for 3D printing is available free from the corresponding authors upon request.

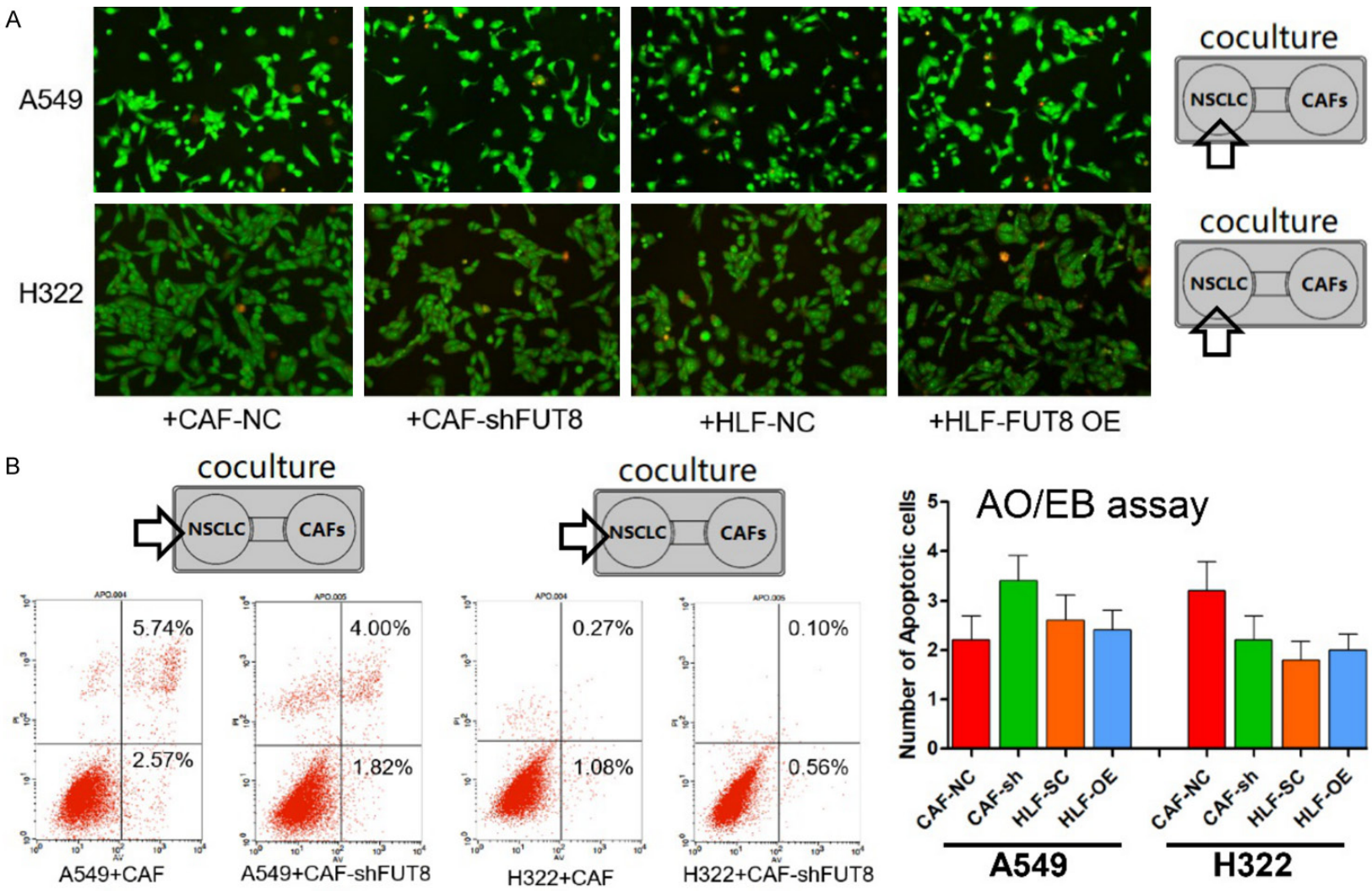
A
A549
H322
coculture
NSCLC
CAFs
coculture
NSCLC
CAFs
+CAF-NC
+CAF-shFUT8
+HLF-NC
+HLF-FUT8 OE
B
coculture
NSCLC
CAFs
coculture
NSCLC
CAFs
5.74%
2.57%
4.00%
1.82%
0.27%
1.08%
0.10%
0.56%
A549+CAF
A549+CAF-shFUT8
H322+CAF
H322+CAF-shFUT8
AO/EB assay
Number of Apoptotic cells
0
1
2
3
4
5
CAF-NC
CAF-sh
HLF-SC
HLF-OE
CAF-NC
CAF-sh
HLF-SC
HLF-OE
A549
H322

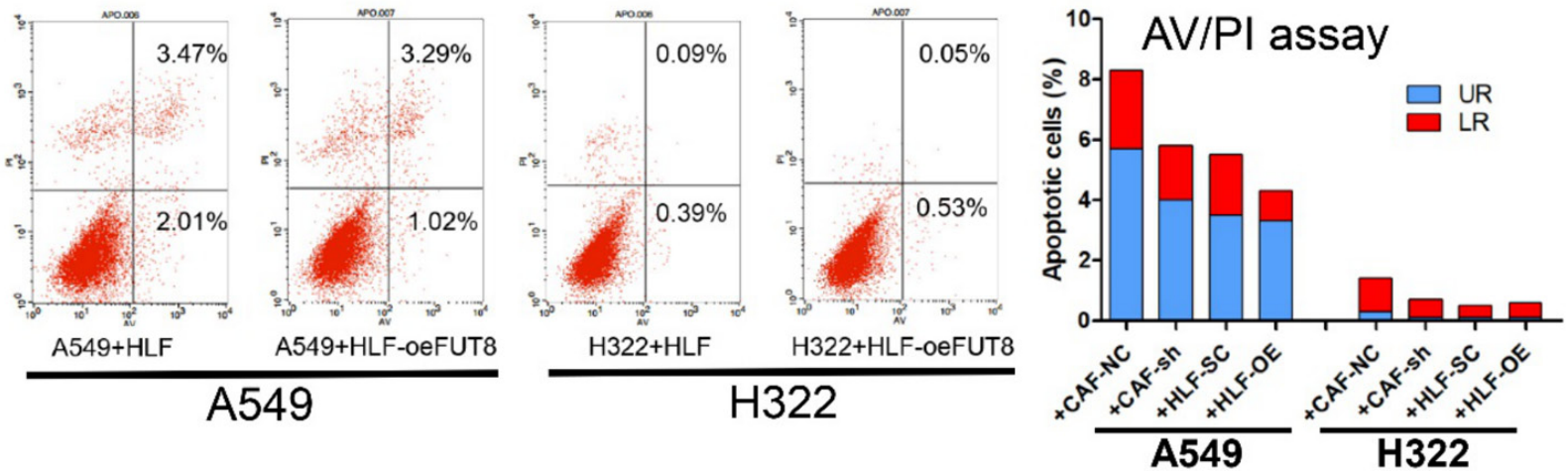

Supplementary Figure 2. A. A549 and H322 cells were co-cultured with fibroblasts in the non-contact co-culture system, and the apoptosis of NSCLC cells was tested by AO/EB staining assays. B. The apoptosis of A549 and H322 cells co-cultured with fibroblasts was tested by AV/PI staining and flow cytometry.

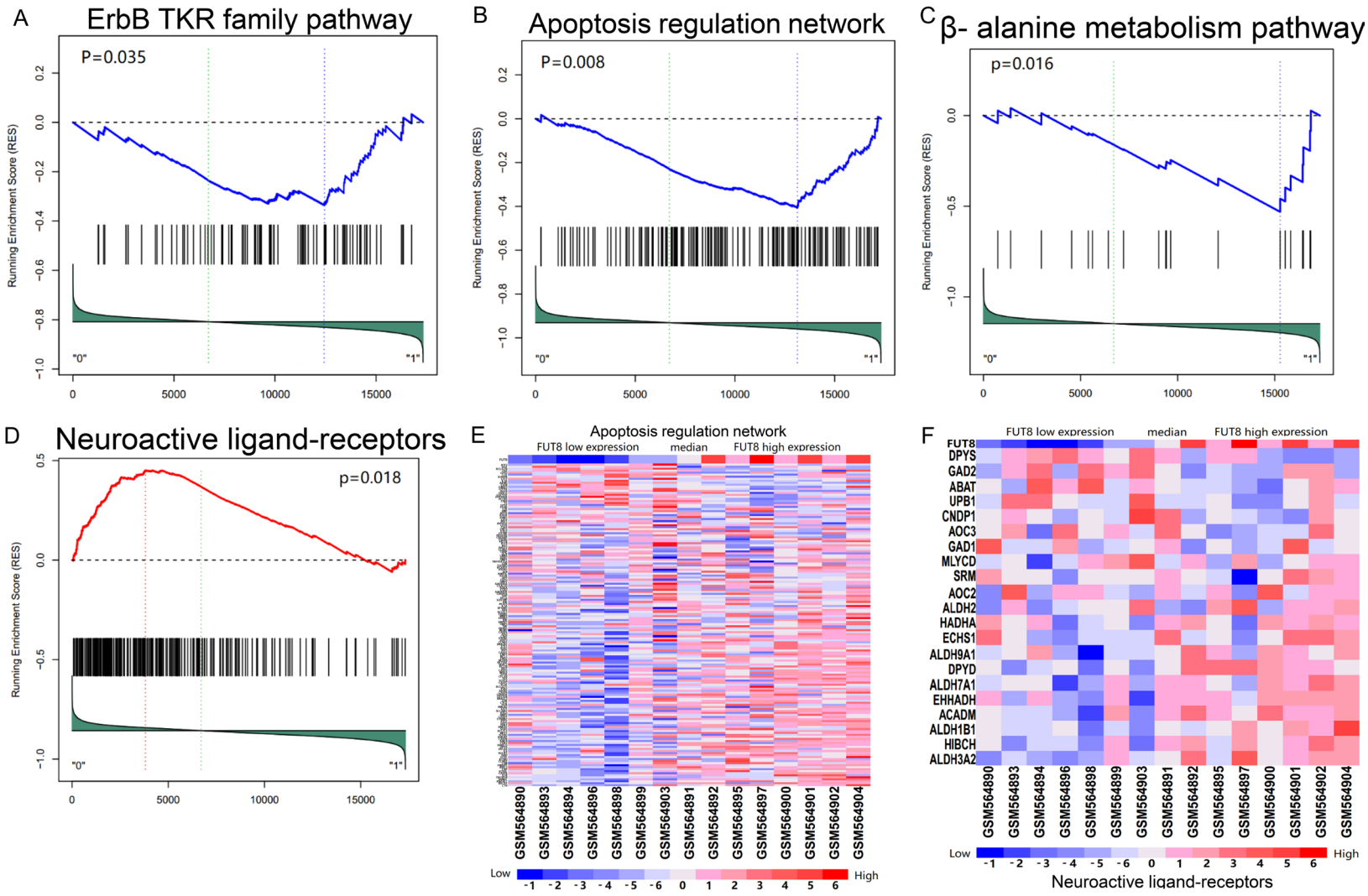
A
ErbB TKR family pathway
P=0.035
B
Apoptosis regulation network
P=0.008
C
β- alanine metabolism pathway
p=0.016
D
Neuroactive ligand-receptors
p=0.018
Running Enrichment Score (RES)
E
Apoptosis regulation network
FUT8 low expression
median
FUT8 high expression
F
FUT8 low expression
median
FUT8 high expression
FUT8
DPYS
GAD2
ABAT
UPB1
CNDP1
AOC3
GAD1
MLYCD
SRM
AOC2
ALDH2
HADHA
ECHS1
ALDH9A1
DPYD
ALDH7A1
EHHADH
ACADM
ALDH1B1
HIBCH
ALDH3A2
Low
High
Neuroactive ligand-receptors

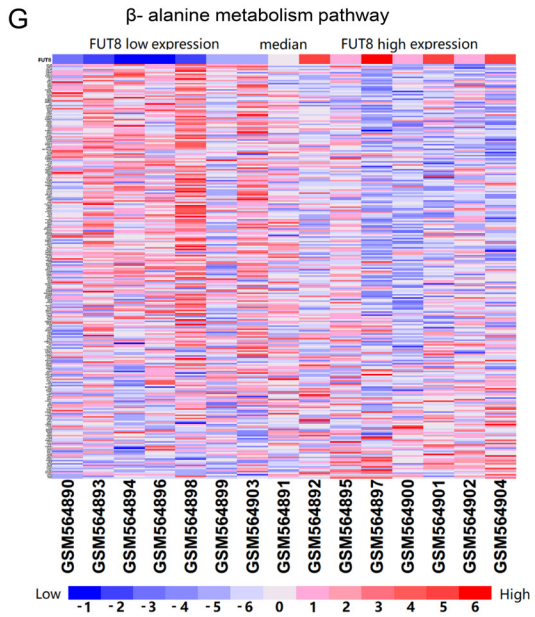

Supplementary Figure 3. A-D. A GSEA revealed the gene list index of the ErbB tyrosine kinase receptor family pathway, the apoptosis regulation network, the β-alanine metabolism pathway, and the neuroactive ligand-receptors. E-G. Heatmaps based on the expression of genes in the three signaling pathways. The colors represent normalized z-scores to illustrate the relative values within rows and cannot be used to compare values between rows. Raw GSEA data are available from the corresponding authors upon request.